Doctorate Dissertation

博士論文

A Patient-derived iPSC Model Revealed the Involvement of Oxidative Stress in Molecular Pathogenesis of Facio-scapulo-humeral Muscular Dystrophy (FSHD)

（ 患者由来 iPS 細胞モデルで明らかとなった
顔面肩甲上腕型筋ジストロフィ(FSHD)における酸化ストレスの病態関与 ）

A Dissertation Submitted for Degree of Doctor of Philosophy
12 2017

平成２９年１２月　博士（理学）申請

Department of Biological Sciences, Graduate School of Science,
The University of Tokyo

東京大学大学院理学系研究科生物科学専攻

Mitsuru Sasaki-Honda

本田（佐々木）充

Abstract

A Patient-derived iPSC Model Revealed the Involvement of Oxidative Stress in Molecular Pathogenesis of Facio-scapulo-humeral Muscular Dystrophy (FSHD)

（ 患者由来 iPS 細胞モデルで明らかとなった
顔面肩甲上腕型筋ジストロフィ(FSHD)における酸化ストレスの病態関与 ）

氏名　本田（佐々木）充

The muscular dystrophies are a group of inherited myogenic diseases that cause progressive skeletal muscle wasting and weakness, and consist of varieties of types with distinct genetic backgrounds and clinical features. In this thesis, I focus on facio-scapulo-humeral muscular dystrophy (FSHD), which is a type of muscular dystrophy strongly associated with epigenetic dysregulation, and aimed at elucidating its pathology.

FSHD is named after muscle areas that are likely to be initially affected, but as symptoms progress, the disease can affect muscles in the whole body, and in some cases patients are forced to use wheel chairs. FSHD patients show unique characteristics of muscle weakness as compared to other types of muscular dystrophies: relatively late onsets of disease phenotypes (typically during the second decade), asymmetric patterns of muscle weakness, and large variations in disease progression among patients. These characteriscs implicate that there are major environmental factors that regulate disease onset and progression even though it is a genetic disease.

DUX4, which is considered as the causative gene of FSHD, is silenced in most of somatic cells in healthy individuals, but is ectopically expressed in the skeletal muscle cells of FSHD patients because of aberrant chromatin relaxation at sub-telomeric region 4q35. The genome at 4q35 in healthy individuals normally contains more than 10 sequential repeat units called D4Z4 which consists of 3.3kp per unit, and forms heterochromatin characterized by DNA hyper-methylation and accumulation of histone 3 lysine 9 tri-methylation (H3K9me3). The diminished heterochromatic state at 4q35 in FSHD patients is caused by either reduced number of D4Z4 repeats (1-10 units) (patients with this case are classified as FSHD type 1, FSHD1) or mutations in genes encoding chromatin regulators, such as *SMCHD1* (structural maintenance of chromosomes flexible hinge domain

containing 1) (patients with this case are classified as FSHD type 2, FSHD2) (Figure.1). However, the mechanism by which *DUX4* expression is regulated remains largely unknown. Furthermore, the low-level expression of *DUX4* raises questions regarding its functional impact, because no report have detected of *DUX4* proteins in muscle biopsies in FSHD patients and because patient-derived primary cultured myoblasts showed low stochastic pattern and distinct levels of *DUX4* expression. In this thesis, I aimed at understanding the pathology in the terms of gene regulation of endogenous *DUX4* expression.

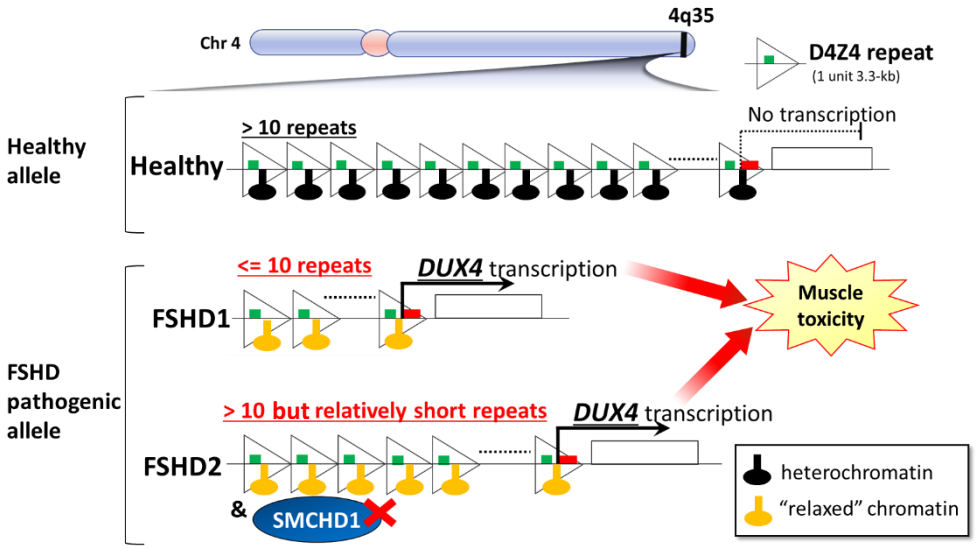

Figure.1 Scheme of genetic backgrounds of FSHD

Induced pluripotent stem cells (iPSCs) opened the door to utilize rare disease patient-derived cellular materials as a feasible and unlimited source for pathological investigation. As FSHD is caused by highly complex genetic backgrounds and the 4q35 genome structure is conserved only in a limited group of primates, patient-derived cells were suitable for FSHD study. Especially, iPSCs are supposed to be more suitable compared to patient-derived primary culture, because primary muscle cultures fundamentally have a limited cell cycle.

To analyze the endogenous *DUX4* expression in patient-derived muscle cells, I established a myocyte model developed from FSHD patient-derived iPSCs. First, iPSC clones were established from a FSHD1 patient (F1), a FSHD2 patient (F2), and a healthy individual (HC) at the laboratory of Dr. Hidetoshi Sakurai, at the Center for iPS Cell Research and Application, Kyoto University. Then by transiently overexpressing MyoD, a master regulator of myogenic linage, the iPSC clones were efficiently differentiated into myosin heavy chain (MyHC) positive myocytes (Figure.2A). Among these myocytes, F1-derived and F2-derived myocytes showed substantial mRNA expression of *DUX4* and its direct downstream targets of *DUX4* transcriptional activity including *ZSCAN4*, but not HC-derived myocytes (Figure.2B). To precisely evaluate the relationship between the genetic background and *DUX4* gene expression, I used genome-editing technology and generated gene-corrected FSHD2-derived clones (isogenic control clones, ICs) by replacing *SMCHD1* mutation with the wild type sequence in F2 iPSC clones. IC-derived myocytes showed suppressed expression of *DUX4* and *ZSCAN4* compared to parental F2-derived myocytes (Figure.2C). These data suggested that the established myocyte model is suitable for further studies of *DUX4* expression.

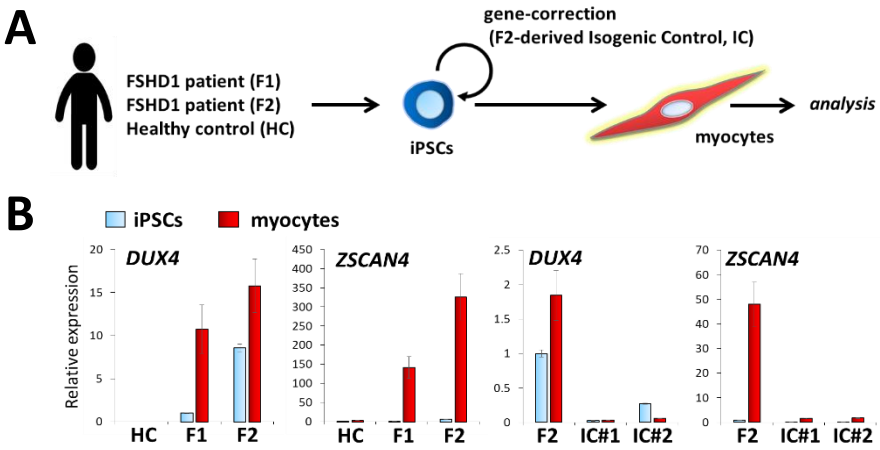

Figure.2 A) A schematic illustration of myocyte model developed from patient-derived iPSCs. B and C) Real-time quantitative PCR (RT-qPCR) analysis for *DUX4* and *ZSCAN4* among iPSCs and myocytes derived from Healthy Control (HC), FSHD1 (F1), FSHD2 (F2), gene-corrected FSHD2 isogenic control (IC#1, IC#2).

Next, I hypothesized that there are extracellular environmental factors that regulate disease progression by altering endogenous *DUX4* expression. As a possible candidate factor, I focus on oxidative stress (OS), which is a common environmental stress in skeletal muscle, because muscle biopsies in FSHD expressed increased markers of OS, and because a small clinical study showed that oral supplementation of antioxidants partially improved muscle function in FSHD patients. Thus, I investigated whether OS can alter *DUX4* expression. By stimulating myocytes of each clone with H_2O_2, which is a model of OS, we determined that *DUX4* expression was specifically increased by OS in both F1 and F2 myocytes (Figure.3). Moreover, gene-corrected IC-derived myocytes showed a marked suppression of OS-induced *DUX4* upregulation (Figure.3), demonstrating that OS-induced *DUX4* increase is a disease-specific molecular phenotype. By chromatin immunoprecipitation (ChIP) analysis, H3K9me3 and HP1γ (heterochromatin protein 1 gamma) were increased at 4q35 in IC-derived

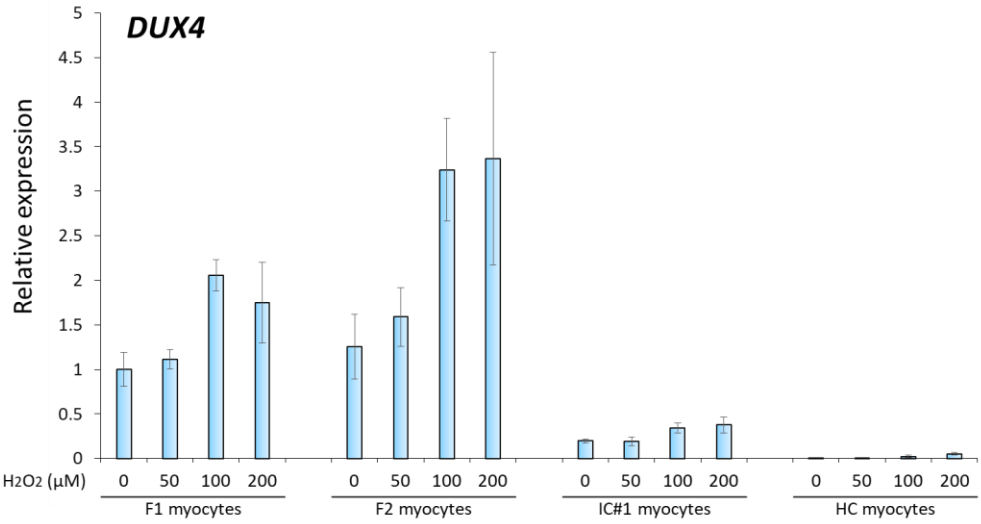

Figure.3 RT-qPCR analysis showed H_2O_2 stimulation induced *DUX4* increase in F1- and F2-derived myocytes and its suppression in gene-corrected IC- and HC-derived myocytes.

myocytes compared to parental F2-derived myocytes, indicating that diminished heterochromatic state in FSHD myocytes permits basal and OS-induced transcription. I further found that DNA damage response (DDR) was involved in OS-induced *DUX4* upregulation and identified ATM (ataxia-telangiectasia mutated kinase), a DDR regulator, as a mediator of this effect. These results suggest that the relaxed chromatin state in FSHD muscle cells permits aberrant access for OS-induced DDR signaling to increase *DUX4* expression (Figure.4).

In conclusion, this new model of FSHD muscle cells developed from patient-derived iPSCs revealed that OS upregulates FSHD-causative *DUX4* through aberrant access of DNA damage response signaling, which is a previously unrecognized mechanism by which *DUX4* expression is regulated in FSHD muscle cells. Thus, OS may represent an environmental risk factor that promotes FSHD progression through *DUX4* gene expression, and this may explain the phenotypic hallmarks of FSHD such as asymmetric patterns of muscle atrophy and varieties of disease progression. This new FSHD model should also provide a basis for drug development and discovery of therapeutic targets for FSHD.

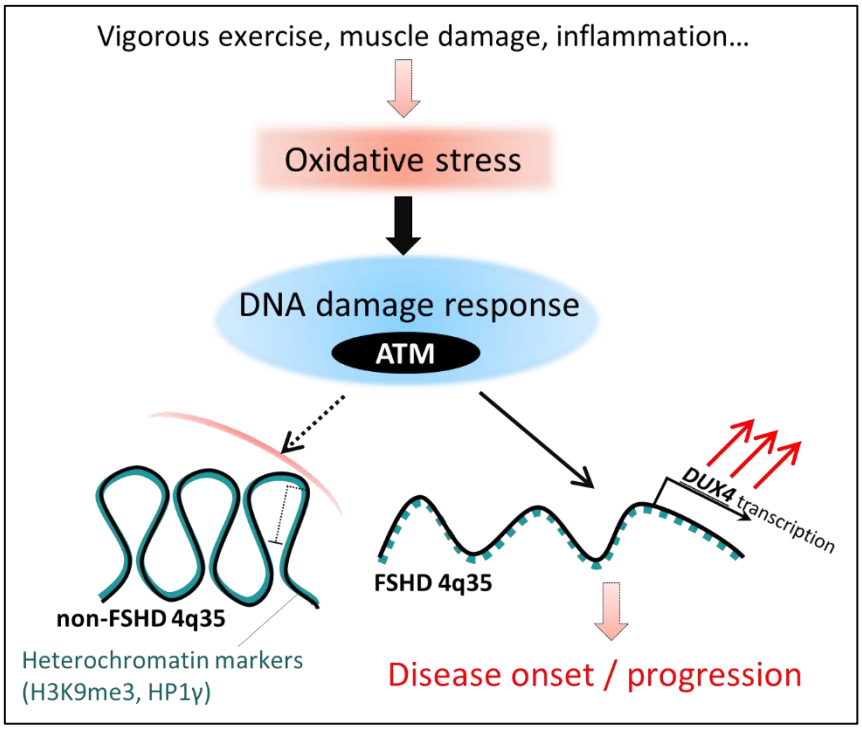

Figure.4 Proposed scheme of involvement of oxidative stress in FSHD pathology propose from this study.

Contents

1. INTRODUCTION

Skeletal muscle is an indispensable tissue that endows animals including human with motility. As skeletal muscle is frequently exposed to varieties of stresses due to its motor function and the environmental or physiological conditions, it possesses high regenerative capacity to recover efficiently and maintain homeostasis. Nevertheless, homeostasis hampered by aging or diseases in human results in muscle degeneration, lowering quality of life and in some cases, threatening lives. The muscular dystrophies are a group of inherited myogenic diseases that cause progressive skeletal muscle wasting and weakness, and consist of varieties of types with distinct genetic backgrounds and clinical features. In this thesis, I focus on facio-scapulo-humeral muscular dystrophy (FSHD), which is a type that is strongly associated with epigenetic dysregulation, and has aimed at elucidating its pathology and to find a clue to cure the patients.

FSHD is named after the muscle areas that are likely to be initially affected, but as symptoms progress, the disease can affect muscle in the whole body and, in some cases, patients are forced to use wheel chairs. FSHD patients show unique characteristics of muscle weakness as compared to other types of muscular dystrophies: relatively late onsets of disease phenotypes (typically during the second decade), asymmetric patterns of muscle weakness, and large variations in disease progression among patients (1). These aspects implicate that there are major environmental factors that regulate disease onset and progression even though it is a genetic disease.

FSHD cases are classified to two subtypes based on the genetic backgrounds. The brief graphical summary is shown in (Figure 1). FSHD type 1 (FSHD1) is caused by reduced D4Z4 repeats (1–10 repeats) followed by a cis-polyadenylation (poly(A)) site at the sub-telomeric region 4q35, whereas FSHD type 2 (FSHD2) is caused

by the presence of mutations in chromatin regulators, including *SMCHD1* (structural maintenance of chromosomes flexible hinge domain containing 1), together with the retention of a normal number of D4Z4 repeats followed by a poly(A) site at 4q35 (2–4). These genomic mutations in both FSHD1 and FSHD2 result in chromatin relaxation at 4q35, which is characterized by DNA hypomethylation and a reduction in the levels of histone 3 lysine 9 trimethylation (H3K9me3) and heterochromatin protein 1γ (HP1γ), and this permits the ectopic expression of *DUX4* (double homeobox 4) transcripts stabilized by a poly(A) signal (4–7). The allele without this poly(A) signal has no potential to ectopic *DUX4* expression; this allows even the individuals harboring reduced numbers of D4Z4 repeats not to manifest FSHD phenotype. Aberrant *DUX4* expression exerts toxic effects in skeletal muscle cells through its transcriptional activity unrelated to muscle function and thus provokes uncontrolled cellular processes (8–10). No clinical difference has been reported between FSHD1 and FSHD2, which are considered to share an identical molecular pathology (11).

The variability in symptoms among FSHD patients is partially explained by an approximate inverse correlation between the number of D4Z4 repeats and clinical severity (12), but the explanation remains incomplete because clinical variability is found even among patients harboring the same number of D4Z4 repeats (13). Based on a series of clinical and genetic studies, the current consensus is that endogenous *DUX4* expression plays a causative role in FSHD pathogenesis; thus, the varying clinical characteristics of the disease strongly support the existence of exogenous factors that modulate the clinical phenotype by affecting events upstream or downstream of *DUX4* expression. Accordingly, a recent study showed that estrogens could function in mediating the sex-related differences in the disease by antagonizing DUX4 downstream events without

altering its expression, and thus protect against impairment of differentiation in patient-derived myoblasts (14). Regarding events upstream of *DUX4*, previous pharmacological studies have identified several upstream regulators of *DUX4* such as Wnt/β-catenin signaling, histone deacetylase (HDAC), PARP1, BRD4, and cAMP-dependent β2-adrenergic receptor signaling (15–18); however, no extracellular factor that increases *DUX4* expression has been reported thus far. Moreover, the low-level expression of DUX4 raises questions regarding its functional impact; only extremely few cultured cells (~1/1000 cells) show detectable DUX4 expression at the translational level (19). Furthermore, to date, no evidence has been reported of DUX4 protein expression in FSHD patient biopsies. However, endogenous DUX4 expression was shown to be sufficient for inducing cellular toxicity during differentiation of myoblasts into myotubes or an impairment of the differentiation of pluripotent stem cells into cells of the skeletal muscle linage (20, 21). Thus, low, but substantial *DUX4* expression in cultured cells derived from distinct patients with FSHD appears to reflect differences in clonal conditions and disease progression of the donors (19). In addition, a recently reported rodent FSHD model showed that the muscular pathological phenotype depends on basal *DUX4* expression levels (22). A consideration of these findings led us to hypothesize that an external factor modulates disease onset and progression in FSHD patients through transcriptional regulation of *DUX4*.

Oxidative stress (OS) is one of the major stresses affecting skeletal muscle function in the context of both homeostasis and pathology (23, 24). The involvement of OS in FSHD pathology is supported by certain clinical and experimental studies. Clinical studies have revealed that OS markers are elevated in FSHD muscle as compared with the level in healthy muscle (25) and that oral supplementation of antioxidants partially improves

muscle function in FSHD patients (26). In addition, results of in vitro experimental studies have shown that FSHD myoblasts are vulnerable to H_2O_2 stimulation, a model of OS, and that DUX4-induced endogenous OS contributes to aberrant differentiation (27–29). Moreover, a series of transcriptomic studies revealed that DUX4 altered the transcription of OS-response genes (30–32). Thus, the findings obtained to date have positioned OS downstream of DUX4 in FSHD pathology; however, no study has investigated whether OS affects *DUX4* expression by acting as an upstream factor.

As FSHD is caused by highly complex genetic backgrounds and the 4q35 genome structure is conserved only in a limited group of primates, patient-derived cells were suitable for FSHD study. Patient-derived primary cells have often been used in that purpose, but limitations still remain because muscle primary cultures fundamentally have a limited cell cycles and patients have to devote the cells from their tissues damaged by their own diseases. Induced pluripotent stem cells (iPSCs) opened the door to utilize rare disease patient-derived cellular materials as a feasible source for pathological investigation of the diseases by their potentials of unlimited self-renewal proliferation (stemness) and differentiation into multiple cell linages (pluripotency) and also by the milder invasive process of their establishment from easily accessible materials such as skin fibroblasts or blood cells (33, 34). Thus, I selected patient-derived iPSCs as a tool for my FSHD study.

In this study, using myocytes differentiated from iPSCs derived from both FSHD1 and FSHD2 patients, I demonstrated that OS increases *DUX4* expression specifically in FSHD muscle cells. By using genome-editing technology, I also generated isogenic controls of FSHD2 iPSCs by correcting the *SMCHD1* mutation; myocytes derived from these isogenic controls showed suppressed basal DUX4 expression and partially recovered

heterochromatic markers at 4q35 and, notably, the OS-induced DUX4 upregulation was also suppressed in these gene-corrected myocytes. Lastly, I attributed the DUX4 upregulation by OS to aberrant access of DNA damage response (DDR) signaling to the opened FSHD 4q35 region, and further identified ATM (ataxia-telangiectasia mutated) kinase as a mediator of this effect. Thus, our results suggest that OS could represent an environmental risk factor that promotes FSHD progression through gene regulation of *DUX4*.

2. MATERIALS AND METHODS

Ethical approval

This study was approved by the Ethics Committee of the Graduate School of Medicine, Kyoto University, and the Kyoto University Hospital (Approval numbers #R0091 and #G259) and was conducted according to the guidelines of the Declaration of Helsinki. To protect confidentiality, all patient information was kept anonymous, and written informed consent was obtained from the study participants.

Cell line and cell culture

Human dermal fibroblasts were donated by one Japanese male FSHD1 patient and one healthy donor. Human blood cells were obtained from one Japanese female FSHD2 patient (35). Donor clinical information is listed in Supplementary Table S1. All human iPSCs used in this study were established by overexpressing four transcription factors by using an episomal vector and were maintained on inactivated mouse feeder cells, as previously described (36), in primate ES cell medium (ReproCELL, Japan) supplemented with 4 ng/mL recombinant human basic fibroblast growth factor (Oriental Yeast, Japan).

Generation of iPS$^{tet\text{-}MyoD}$ clones

The MyoD element was cloned into the PB-TAC-ERN vector by using Gateway cloning to generate PB-MyoD as previously described (36). iPSCs were transfected with plasmids, including PBase and PB-MyoD, by using a NEPA21 electroporator (Nepagene, Japan) and plated on mouse feeder cells for clone selection and culture maintenance as previously described (36).

Myocyte differentiation

iPS$^{tet\text{-}MyoD}$ cells were treated with accutase (Nacalai Tesque, Japan) to separate them into single cells and were plated at a density of 3–5 × 10^5 cells/well in 6-well dishes coated with Matrigel (BD Biosciences, USA); the cells were plated in primate ES cell medium supplemented with 100 μg/mL neomycin sulfate (Nacalai Tesque) and 10 μM Y-27632 (Nacalai Tesque). On the following day, the culture medium was replaced with primate ES cell medium containing 1–2.5 μg/mL doxycycline (Dox; LKT Laboratories, USA). Induction was performed in 5% KSR/α-MEM containing Dox and 2-mercaptoethanol (2-ME) supplement for 5–7 days.

Correction of *SMCHD1* mutation in iPSCs

The mutation in *SMCHD1* was corrected through homologous recombination (HR)-mediated knock-in using the CRISPR/Cas9 system (clustered regularly interspaced short palindromic repeats (CRISPR) and CRISPR associated 9 (Cas9) endonuclease system) as described (37). Briefly, the single-guide RNA (sgRNA) sequence was designed for an intron site near the mutation site by using CRISPRdirect online software (http://crispr.dbcls.jp/) (38) and cloned into pHL-H1-ccdB-mEF1a-RiH. For the HR template, bilateral ~1-kb regions interposing the sgRNA target site, with the mutation in exon 32 replaced by the wild-type sequence, were cloned and inserted before and after the puromycin-resistance gene element with two loxP sites in pENTR-Donor-MCS2. The sgRNA vector, the HR vector, and pHL-EF1a-SphcCas9-iP-A were co-transfected, using a NEPA21 electroporator, into F2 iPS$^{tet\text{-}MyoD}$ cells, and then subcloning was performed after drug selection for 1 week. Among the obtained clones, those harboring the homozygous HR-derived sequence were selected and transfected with a Cre recombinase construct, and subcloning was again performed to select the clones that had lost the puromycin resistance. Lastly, the sequence was confirmed to contain only one loxP site in each allele.

The primers used in these procedures are listed in Table 2.

Knockdown using short-hairpin RNA (shRNA)

The U6 promoter with a termination site in BLOCK-iT™ U6 RNAi Entry Vector (Invitrogen, USA) was transferred to the piggyBac vector. The sequences listed in Table 3 were annealed and inserted after the U6 promoter. Each vector was transfected into the F1 iPS$^{tet\text{-}MyoD}$ clone by using the NEPA21 electroporator as described above.

Immunofluorescence analysis

Cultured cells were fixed with 2% formaldehyde in PBS, washed in PBS, re-fixed with 100% methanol, and blocked with Blocking One solution (Nacalai Tesque) at 4 °C. Fixed samples were incubated overnight at 4 °C with primary antibodies diluted in 10% Blocking One/PBST (PBS containing 0.2% Triton X-100 (Santa Cruz, USA)), washed repeatedly with PBST, and incubated for 1 h with secondary antibodies (diluted in 10% Blocking One/PBST) and the nuclear stain DAPI (Sigma; 1:5000). Samples were examined and images were captured using a BZ9000 system (Keyence, Japan) at 200× and 400× magnification. The antibodies used in this study are listed in Table 4.

RNA extraction and real-time reverse-transcription quantitative PCR (RT-qPCR)

Total RNA was extracted using a ReliaPrep RNA Miniprep System (Promega), as per the manufacturer's instructions; subsequently, cDNA was synthesized from the extracted RNA by using ReverTra Ace Master Mix with gDNA Remover (TOYOBO, Japan) or a Superscript III First-Strand Synthesis system for RT-PCR (Invitrogen) with random hexamers as primers after treatment with DNaseI (Invitrogen) to remove genomic

DNA for long non-coding RNA (lncRNA) detection. Real-time RT-qPCR was performed using SYBR Green probe sets (Applied Biosystems) and a Step One Plus thermal cycler (Applied Biosystems), and a standard curve was prepared for each target, except in the case of the assays presented in Figures 1E-1G and 3F-3H, where data were quantified using the ΔΔCt method. *RPLP0*, which encodes a ribosomal protein, was used as the internal control in all assays except those shown in Figures 1E-1G and 3F-3H, where *ACTB* served as the internal control. The primer sets used in this study are listed in Table 5.

Chromatin immunoprecipitation (ChIP) and ChIP qPCR analysis

ChIP analysis was performed by using an EpiScope ChIP Kit (TAKARA, Japan) according to the manufacturer's instructions with partial modifications. Briefly, 2–5 × 10^6 cells of each iPSC clone were plated and differentiated in 10-cm dishes to obtain equally confluent myocytes. The cells were crosslinked for 5 min at room temperature with 1% formaldehyde and lysed, and the lysates were sonicated with a Bioruptor (BM EQUIPMENT, Japan) for 12 cycles (high intensity, 30/30-s on/off per cycle). Fragmented lysates were incubated with antibodies conjugated to mouse IgG magnetic beads (TAKARA) or Dynabeads Protein G (Thermo Fisher Scientific, USA) overnight, washed with a series of buffers, and immunoprecipitated, and 10% of the input chromatin was purified by reversing the crosslink and treating with RNase A and Proteinase K. RT-qPCR followed by the ΔΔCt method was used to quantify the D4Z4 elements. Relative %input was calculated by dividing the amount of immunoprecipitated chromatin by that of the input and then normalizing relative to the F2 sample. The following primer pair was used for D4Z4 elements: 5′-CCGCGTCCGTCCGTGAAA-3′ and 5′-TCCGTCGCCGTCCTCGTC-3′ (5).

DNA methylation analysis

Genomic DNA was extracted using a GenElute Mammalian Genomic DNA Miniprep Kit (Sigma-Aldrich, USA), as per the manufacturer's protocol; 500 ng to 1 μg of DNA was treated with bisulfite by using an EpiTect DNA bisulfite kit (QIAGEN, Germany) according to manufacturer guidelines. For the F1 clone, the methylation level of the FSHD allele was quantified using the pyrosequencing technique as described in (35). Briefly, PCR was performed using a PyroMark PCR Kit (QIAGEN), and 10 μL of the biotinylated PCR product was affinity purified using Streptavidin Sepharose High Performance (GE Healthcare Life Science, UK) and PyroMark Q24 Advanced CpG Reagents (QIAGEN). For the F2 isogenic controls IC#1 and IC#2, PCR and DNA methylation analysis of the 4qA distal region were performed according to the protocol of the 4qA BSS assay as described in (39) for QUMA online software (http://quma.cdb.riken.jp/index_j.html) (40); the analysis was performed using the default parameters.

Reagents

Hydrogen peroxide mixed with a stabilizer (H_2O_2, Sigma) was added at various concentration by diluting a 1 mM stock immediately before use on Day 8 of myocyte differentiation after depletion of 2ME for one day. N-acetylcysteine (NAC) was dissolved in water and the pH was adjusted to 7.0, and NAC was added to cells 1 h before H_2O_2 stimulation. KU-55933 (Selleck Chemicals, USA), VE-821 (AdooQ BioScience, USA), NU-7441 (Selleck Chemicals), PD0325901 (Cayman Chemical, USA), SP600125 (Selleck Chemicals), and SB203580 (Sigma) were dissolved in DMSO (Sigma) and were added 1 h before H_2O_2 stimulation. Mitomycin C was added at various concentration for two hours and then washed once and replaced by medium.

UV-C irradiation

For the light source of UV-C, the lamps inside the laminar flow cabinet were used. Myocytes that were differentiated on 6-cm dishes were washed once and medium was replaced by PBS. Myocytes were then positioned on a fixed position inside the laminar flow cabinet, exposed to UV-C, and then washed once and PBS was replaced by medium.

3. RESULTS

Generation of iPS$^{tet\text{-}MyoD}$ clones from FSHD1 and FSHD2 patients and healthy control donor

I prepared iPSCs from one FSHD1 patient harboring 3 D4Z4 repeats (F1), one FSHD2 patient harboring a *SMCHD1* mutation (F2), and one healthy donor with no FSHD symptoms (HC) by using a previously established method, in which episomal vectors carrying the reprogramming factors Oct3/4, Sox2, Klf4, and L-Myc were transfected into skin fibroblasts of HC and F1 and blood cells of F2 (Table 1). To obtain iPSCs possessing the potential to efficiently differentiate into myocytes, I used a tetracycline-inducible MyoD piggyBac vector (tet-MyoD) that was constructed previously; this enabled the transfected iPSCs (iPS$^{tet\text{-}MyoD}$) to express MyoD, a master regulator gene for skeletal muscle differentiation, and subsequently differentiate into myosin heavy chain (MyHC)-positive myocytes only when Dox was added to the medium (Figure 2) (36). The expression of stage-specific embryonic antigen (SSEA)-4 and tumor-related antigen (TRA)-1–60, which are indicators of undifferentiated pluripotent stem cells, was detected by immunocytochemistry, and this demonstrated that the iPS$^{tet\text{-}MyoD}$ clones retained undifferentiated pluripotent characteristics (Figure 3A). To model myocytes, myogenic differentiation was performed on these iPS$^{tet\text{-}MyoD}$ clones through Dox-inducible MyoD overexpression. On Day 8, >80% of the nuclei were positioned inside MyHC-positive cells in each clone, which indicated that a comparable myocyte lineage was induced from HC, F1, and F2 iPS$^{tet\text{-}MyoD}$ clones (Figure 3B and 3C). The results of RT-qPCR analysis for pluripotency markers *(OCT3/4*, *NANOG*, and *SOX2*) and muscle-linage markers (*MYOG*, *MYH3*, and *CKM*) confirmed efficient myogenic differentiation of each cell line (Figure 4A and 4B). Moreover, RT-qPCR analysis for *DUX4* and its reported downstream targets (*ZSCAN4*,

TRIM43, and *MBD3L2*) revealed considerably higher expression of these molecules in the differentiated state than in the undifferentiated state in the F1 and F2 clones but not in the HC clone (Figure 4C). In the case of the F1 clone, DNA methylation analysis specific for the allele harboring short D4Z4 repeats revealed that DNA methylation was stably low during the reprogramming from fibroblasts to iPSCs or differentiation from iPSCs to myocytes, as compared to the healthy level (>26%) reported previously by using the same methods (Figure 5) (35). These data suggested that the myocytes that were differentiated from human iPSC clones were suitable for investigating FSHD-related *DUX4* expression.

OS increased DUX4 expression in both FSHD1 and FSHD2 myocytes

To investigate whether OS increases *DUX4* expression, I stimulated myocytes with H_2O_2, which served here as an OS model. RT-qPCR analysis of *DUX4* mRNA expression in myocytes showed that H_2O_2 stimulation for 24 h significantly increased *DUX4* transcription in a dose-dependent manner, which was not observed in the healthy control (Figure 6A). To confirm this DUX4 upregulation at the protein level, the transcription of *ZSCAN4*, a direct downstream target of DUX4 transcriptional activity, was analyzed using RT-qPCR; the results indicated that H_2O_2 stimulation also increased DUX4 expression at the translational level (Figure 6B). Conversely, treatment with NAC, an antioxidant, attenuated the *DUX4* increase induced by H_2O_2, which indicated that the OS caused by H_2O_2 stimulation was responsible for *DUX4* upregulation (Figure 6C). Time-course analysis further revealed that the upregulation of *DUX4* transcription started between 6 and 12 h after H_2O_2 stimulation, which suggested that an early response to OS mediates the increase in transcription (Figure 6D). These myocytes of each clone under H_2O_2 stimulation survived for 24 h, indicating that the oxidative stress

physiologically mild to allow cell survival can induce *DUX4* increase in FSHD muscle cells (Figure 7). By contrast, *DUX4* was not expressed in F1 fibroblasts in a transcriptional or a translational level in the presence or absence of H_2O_2 stimulation (Figure 8A and 8B). These data demonstrated that OS increased *DUX4* expression in FSHD muscle cells.

***DUX4* expression in F2 isogenic control clones showed basal suppression and resistance to OS**

To ascertain whether the OS-induced *DUX4* upregulation was a disease-specific event, I generated isogenic control cell lines by correcting the *SMCHD1* mutation in F2 $iPS^{tet\text{-}MyoD}$ cells by using the CRISPR/Cas9 system together with donor template vectors for homology-directed repair (Figure 9A). The patient F2 carried a heterozygous 15-bp frameshift mutation with a 1-bp substitution in exon 32 of *SMCHD1*, which was modified to generate two isogenic clones (IC#1 and IC#2) in which the mutations were replaced with the wild-type sequence (Figure 9A and 9B). Immunochemistry showed that these isogenic clones retained the expression of pluripotency markers and exhibited comparable ability to differentiate into MyHC-positive myocytes, indicating those isogenic controls were suitable for further comparison to parental F2 clone (Figure 10A-10C). Gene expression analysis also showed efficient differentiation from iPSC state into myocytes for each clone (Figure 11A-11B). In IC#1 and IC#2 myocytes, *DUX4* and its downstream targets were expressed at substantially lower levels than in the parental clone F2 myocytes, which indicated that the *SMCHD1* mutation was responsible for the basal *DUX4* transcription in these F2 myocytes (Figure 11C). Moreover, the myocytes differentiated from the isogenic control clones showed only a slight increase in *DUX4* expression following H_2O_2 stimulation, and the expression level in the isogenic control IC#1 myocytes treated with the highest concentration of H_2O_2 was

still lower than that in the parental clone without stimulation (Figure 12A-12C). The similar tendency was also observed in another isogenic control IC#2 myocytes (Figure 13A-13B). These data indicate that the *DUX4* expression level and its marked increase induced by OS were dependent on the disease-causing *SMCHD1* mutation in FSHD2.

Heterochromatic status at 4q35 was partially increased in F2 isogenic control myocytes

FSHD 4q35 is characterized by chromatin relaxation: DNA hypomethylation and reduced levels of H3K9me3 and HP1γ (5, 6). Unexpectedly, DNA methylation in the 4qA allele was not increased shortly after the gene correction in IC#1 myocytes (Figure 14A). However, ChIP followed by RT-qPCR analysis revealed that the accumulation of H3K9me3 and HP1γ was increased in D4Z4 regions in the IC#1 myocytes, whereas H3K4me2 was not significantly increased (Figure 14B). Moreover, SMCHD1 accumulation was also increased in IC#1 myocytes, indicating *SMCHD1* haploinsufficiency in the F2 clone (Figure 14B). The similar tendency was also observed in another isogenic control IC#2 myocytes (Figure 15A-15B). These data indicated that a reduction of heterochromatic histone modification underlay *DUX4* basal expression and upregulation by OS in FSHD myocytes.

***DUX4*-upstream lncRNA played a major role in basal regulation of *DUX4* expression but a minor role in its increase induced by OS**

Next, to investigate the events upstream of OS-induced increase in *DUX4*, I examined the expression of the disease-associated lncRNA DBE-T, which was shown to regulate *DUX4* transcription (41). DBE-T was also increased upon H_2O_2 stimulation in the clones derived from the FSHD patients, but not in the healthy clone or

in an FSHD2 isogenic control clone (Figure 16A-16C). To determine whether this DBE-T increase was responsible for *DUX4* upregulation, DBE-T knockdown was performed through shRNA delivery by using a piggyBac vector, which did not affect differentiation efficiency in $iPS^{tet\text{-}MyoD}$ clones (data not shown). DBE-T knockdown was confirmed using RT-qPCR (Figure 17A). Partial suppression of DBE-T expression attenuated the basal *DUX4* expression and the increase in expression induced by H_2O_2, but the ratio of the increase was not altered (Figure 17B and 17C). These data confirmed a correlation between the expression of DBE-T and *DUX4* in the presence and absence of OS stimulation, but DBE-T does not appear to play a major role as an inducer of *DUX4* upregulation under OS.

DDR occurred before *DUX4* upregulation under OS

I also investigated whether DDR was involved in OS-induced increase in *DUX4*, because H_2O_2 stimulation exerts a broad range of effects on cells, including DNA damage (23, 42). At 6 h after H_2O_2 stimulation, when *DUX4* expression was not yet affected by H_2O_2 (Figure 6D), the expression of γ-H2AX, an indicator of DDR, showed H_2O_2 dose-dependent increase in F1 myocytes (Figure 18A and 18B). Moreover, because UV-C exposure induces DDR, I examined its effect, and found that short exposure of F1 myocytes to UV-C, which allowed most of the cells to survive for 24 h, also upregulated *DUX4* expression (Figure 19A-19C). Lastly, to determine whether DNA damage alone is sufficient to induce *DUX4* increase, F1 myocytes were treated with mitomycin C, a DNA damage inducer, and this treatment also upregulated *DUX4* expression (Figure 20A and 20B). These data indicated that *DUX4* increase induced by OS is mediated by DDR.

OS indirectly upregulated *DUX4* through ATM-mediated DDR

DDR is primarily controlled by three phosphoinositide 3-kinase-related kinases: ATM, ATR (ATM and Rad3-related), and DNA-PK (DNA-dependent protein kinase) (43, 44). To identify the kinase that is responsible for OS-induced *DUX4* upregulation, F1 myocytes were stimulated with H_2O_2 in the presence and absence of specific kinase inhibitors: Whereas inhibition of ATR or DNA-PK did not markedly affect *DUX4* expression, ATM inhibition attenuated *DUX4* upregulation induced by H_2O_2 in a concentration-dependent manner (Figure 21A). Moreover, treatment with the ATM inhibitor caused a decrease in the number of γ-H2AX-positive nuclei under the OS condition in F1 myocytes, which indicated that the DDR triggered by H_2O_2 stimulation was prevented by ATM inhibition (Figure 21B and 21C). Although OS can directly activate members of the stress-induced MAP kinase family (23, 45), inhibition of MEK, JNK, or p38 MAPK did not suppress OS-induced *DUX4* upregulation; therefore, this upregulation appeared to be an indirect outcome produced through DDR (Figure 23). Lastly, the *DUX4* increase in F2 myocytes under the OS condition was also attenuated by the ATM inhibitor (Figure 22D). Thus, these data indicated that ATM mediates the OS-induced *DUX4* upregulation in FSHD myocytes.

4. DISCUSSION

FSHD is caused by genetic disorders but patients show variations in disease progression; this suggests the existence of certain external factors that modulate the pathological condition of FSHD. To our knowledge, this study has demonstrated for the first time that the expression of *DUX4*, the gene widely accepted to be primarily responsible for FSHD pathology, is upregulated by external cellular stress. Furthermore, I have shown that the *DUX4* increase induced by OS is mediated by the DDR signaling pathway, which suggests that diverse types of genotoxic stress can cause an increase in *DUX4* expression and could therefore represent risk factors for FSHD onset or progression.

The involvement of OS in FSHD pathology has been previously reported by several groups. DUX4-expressing muscle cells showed transcriptome enrichment in OS-related gene expression (30–32). Moreover, exogenous *DUX4* expression in mouse myoblasts or human immortalized myoblasts resulted in vulnerability to OS (28, 46), and endogenous *DUX4* expression in immortalized FSHD myoblasts also led to vulnerability to OS and provoked endogenous reactive oxygen species (ROS) production followed by DDR to partial failure in differentiation (29). Intriguingly, all these findings on the association of OS with FSHD provide insights into the downstream consequences of *DUX4* expression. By contrast, our results here suggest another potential role of OS and DNA damage in FSHD, as upstream inducers of *DUX4* expression. Collectively, these findings indicate that a positive-feedback loop of signaling cascades could be formed among OS, DNA damage, and endogenous *DUX4* expression. During myogenic differentiation in mouse and human myoblasts, transient DNA strand breakage occurs followed by the formation of γ-H2AX foci (47, 48), and this might underlie the “burst”

of DUX4 expression in a limited population of FSHD myoblasts during differentiation (20). In the context of differentiated muscle cells, which are recognized to be resistant to diverse stressors (49, 50), including H_2O_2 and DNA damage inducers, DNA damage can be accumulated without cell death by preventing the p53-mediated apoptosis pathway (49, 50). This might contribute to the increase in *DUX4* expression induced in muscle fibers by OS and other genotoxic stresses. Thus, OS and DNA damage are likely to influence FSHD pathology through the regulation of *DUX4* expression.

ATM performs multiple functions in DDR signaling at DNA lesion sites, including transcriptional regulation and DNA repair. Here, I propose that the diminished heterochromatic state at the 4q35 region, characterized by a reduction of H3K9me3 and HP1γ, increases the region's sensitivity to DNA damage-induced ATM activity, which results in *DUX4* upregulation (Figure 8). A considerable amount of evidence has implicated chromatin compaction in the regulation of ATM activity. HDAC inhibition in human fibroblasts permitted ATM-mediated transcriptional upregulation of MCL1 and Gadd45α, which are ATM targets, through recruitment of E2F1 transcription factor (51). In the context of DNA repair, heterochromatin serves as a barrier to the expansion of ATM-dependent γ-H2AX (52, 53). Moreover, a decrease in chromatin compaction, which was induced by reducing the level of linker histone H1, enhanced resistance to DNA damage through increased accessibility of DDR factors to lesion sites (54). Thus, I suggest that the non-FSHD 4q35 region is transcriptionally silenced and is less sensitive to the DNA damage-induced ATM-mediated transcriptional machinery, whereas FSHD 4q35 permits the ATM-mediated machinery to access the lesion site (Figure 23).

Notably, our FSHD models showed that the expression of *DUX4* and its downstream targets was

fundamentally dependent on myogenic differentiation and disease-related mutation in *SMCHD1* (Figures 4C and 11C), which indicates that our FSHD models are useful for further FSHD pathological studies. Isogenic controls generated for the FSHD2 clone showed robust suppression of endogenous *DUX4* expression, which clearly agrees with previous genetic studies (7); moreover, our results also provide certain intriguing insights. First, whereas the F1 clone showed myocyte-specific *DUX4* expression and activity, the F2 clone, even in the iPSC state, expressed *DUX4* without the expression of its downstream targets (Figure 4C); this finding indicates that endogenous DUX4 (not that from the overexpression construct) alone cannot sufficiently activate downstream targets in the iPSC state and might require certain transcriptional co-regulators that exist in the muscle linage but not in the iPSC state. This notion is supported by the function of the DUX4 C-terminal region as a transactivation domain recruiting co-activators, which is necessary for inducing cytotoxicity (55). Second, SMCHD1 was found to recover the heterochromatic state according to the level of a protein marker (although the level was still lower than that in the healthy control; data not shown) but not in terms of the DNA methylation level (Figure 14 and 15); this indicates that the DNA methylation status, once determined, remains stable and resistant to post-developmental modification by epigenetic factors, whereas alterations of heterochromatic protein markers are sufficient to suppress *DUX4* expression at 4q35, which agrees with the finding that H3K9me3 was not hampered by DNA demethylation at 4q35 (5). This supports the modification of histone markers as a therapeutic strategy for FSHD.

Although the FSHD myocytes used in our study expressed *DUX4* to the extent that upregulated downstream transcriptional targets, I did not observe marked phenotypic changes, including apoptosis or impaired

differentiation, as previously reported (15, 21). I propose two possible reasons for this phenotypic absence: one, the survival duration of our FSHD myocyte models might be insufficiently long to allow the induction of notable phenotypic changes under the mild OS conditions used in this study. In this scenario, the *DUX4* increase induced by OS might provoke certain changes under a higher H_2O_2 concentration, but these cannot be readily recognized as DUX4-specific effects because stronger H_2O_2 treatment can induce cell death independently of DUX4 (Figure 7). To overcome this challenge, a more mature muscle linage showing longer survival must be used to evaluate how long-term treatment with mild OS affects FSHD muscle cells through *DUX4* expression. Two, the myocytes induced in our model system, which was shown to mimic the embryonic myogenic linage, might maintain resistance to DUX4 activity. Given that *DUX4* expression is detected even in the FSHD embryo and that the disease phenotypes are manifest long after birth in most FSHD cases (56), embryonic myocytes might be capable of tolerating DUX4 expression. For investigating this possibility, the “adult state” of muscle cells could be useful.

5. CONCLUSION

In accordance with previous studies and from a novel point of view, my findings indicate that increased OS is a risk factor for FSHD patients. As OS can occur locally in the body, my finding that positon OS as an upstream regulator of *DUX4* gene expression may explain some of FSHD hallmarks such as asymmetric muscle atrophy or preference of affected muscle areas. This elevated OS could potentially be attenuated through supplementation with ROS scavengers or even by including antioxidative nutrients in the daily diet. In summary, my study has revealed, by using patient-derived iPSCs, a previously unrecognized mechanism by which *DUX4* expression is regulated in FSHD muscle cells, and this should provide a basis for drug development and discovery of therapeutic targets for FSHD.

6. TABLES AND FIGURES

Table 1. Information of each donor for establishment of iPS clones

Donor	Type	Sex	Number of D4Z4 repeats on 4qA allele	SMCHD1 mutation	Age of onset (yrs)	Age of specimen provided (yrs)	origin of cell
F1	FSHD1	Male	3	–	13	26	skin fibroblasts
F2	FSHD2	Female	12	heterozygous g.2750458_2750472del	14	55	blood cells
HC	–	Female	N.D.	–	–	35	skin fibroblasts

Table 2. Primers used in gene modification.

Purpose		
Arm region for HR template	Fw	GAAAGTGAAAGCTTGGTTATCACTG
	Rv	GAAACATCACAATGTAGACTACTC
PCR amplicon for sequencing	Fw	GAGATGGGTTTTAGGATTTGGGAGAA
	Rv	TCCACTCTCTTTCAAGCAGTCTATCA

Table 3. Primers for shRNA constructs

Target		Sequence	Ref
Control	Fw	GATCCGCAACAAGATGAAGAGCACCAACGAATTGGTGCTCTTCATCTTGTTGTTTTTT	
	Rv	CTAGAAAAAACAACAAGATGAAGAGCACCAATTCGTTGGTGCTCTTCATCTTGTTGCG	
DBE-T	Fw	GATCCGGCTCACCGCCATTCATGAAGGCGAACCTTCATGAATGGCGGTGAGCTTTTTT	
	Rv	CTAGAAAAAAGCTCACCGCCATTCATGAAGGTTCGCCTTCATGAATGGCGGTGAGCCG	

Table 4. Antibodies used in this study.

1st Antibody	Source	Clonarity	Dilution	Company
Myosin Heavy Chain (MyHC, MF20)	Mouse	Monoclonal	1/800	eBiosciencce
Stage-Specific Embryonic Antigen-4	Mouse	Monoclonal	1/100	Millipore
TRA-1-60	Mouse	Monoclonal	1/100	Millipore
γ-H2AX (N1-431)	Mouse	Monoclonal	1/800	BD Biosciences
2nd Antibody	Dilution	Company		
Alexa Fluor 488 anti-mouse IgG	1/500	invitrogen		
Alexa Fluor 488 anti-mouse IgG2b	1/500	invitrogen		
Alexa Fluor 568 anti-mouse IgG1	1/500	invitrogen		

Table 5. Primer sets for RT-qPCR analysis in this study.

	Target		Sequence		PCR condition			Ref
RT-qPCR	ACTB	Fw	CTCTTCCAGCCTTCCTTCC		Denature	95℃	15″	
		Rv	CACCTTCACCGTTCCAGTTT		Anealing	60℃	60″	
	RPLP0	Fw	AAACGAGTCCTGGCCTTGTCT		Denature	95℃	15″	
		Rv	GCAGATGGATCAGCCAAGAAG		Anealing	60℃	60″	
	OCT3/4	Fw	GACAGGGGGAGGGGAGGAGCTAGG		Denature	95℃	15″	
		Rv	CTTCCCTCCAACCAGTTGCCCCAAAC		Anealing	60℃	60″	
	NANOG	Fw	CAGTCTGGACACTGGCTGAA		Denature	95℃	15″	
		Rv	CTCGCTGATTAGGCTCCAAC		Anealing	60℃	60″	
	SOX2	Fw	GGGAAATGGGAGGGGTGCAAAAGAGG		Denature	95℃	15″	
		Rv	TTGCGTGAGTGTGGATGGGATTGGTG		Anealing	60℃	60″	
	MYOG	Fw	TGGGCGTGTAAGGTGTGTAA		Denature	95℃	15″	
		Rv	CGATGTACTGGATGGCACTG		Anealing	60℃	60″	
	MYH3	Fw	GCAGATTGAGCTGGAAAAGG		Denature	95℃	15″	
		Rv	TCAGCTGCTCGATCTCTTCA		Anealing	60℃	60″	
	CKM	Fw	ACATGGCCAAGGTACTGACC		Denature	95℃	15″	
		Rv	TGATGGGGTCAAAGAGTTCC		Anealing	60℃	60″	
	DUX4	Fw	CCTGGGATTCCTGCCTTCTA		Denature	95℃	30″	
		Rv	AGCCAGAATTTCACGGAAGA		Anealing	62℃	45″	
	ZSCAN4	Fw	GTGGCCACTGCAATGACAA		Denature	95℃	15″	
		Rv	AGCTTCCTGTCCCTGCATGT		Anealing	60℃	60″	
	MBD3L2	Fw	CGTTCACCTCTTTTCCAAGC		Denature	95℃	15″	
		Rv	AGTCTCATGGGGAGAGCAGA		Anealing	60℃	60″	
	TRIM43	Fw	ACCCATCACTGGACTGGTGT		Denature	95℃	15″	
		Rv	CACATCCTCAAAGAGCCTGA		Anealing	60℃	60″	
	DBE	Fw	AGGCCTCGACGCCCTGGGTC		Denature	95℃	15″	
		Rv	TCAGCCGGACTGTGCACTGCGGC		Anealing	60℃	60″	
	DBE(NDE)	Fw	AGGCAAAATCCTCCCAGAATC		Denature	95℃	15″	
		Rv	CCATCTCCCCTCACACACTT		Anealing	60℃	60″	

Figure 1. Scheme of genetic backgrounds of FSHD.

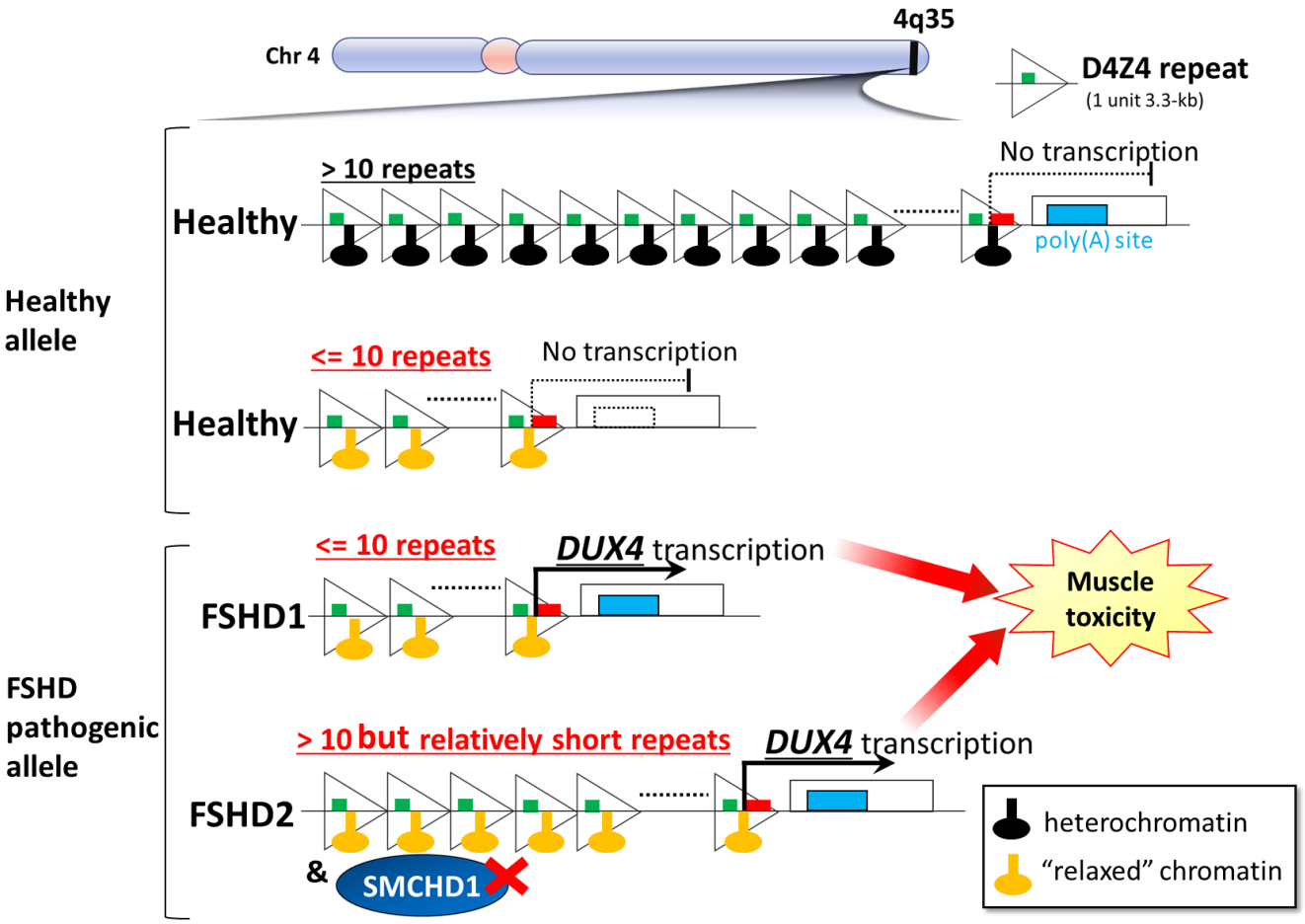

Figure 2. Scheme of differentiation of iPSC clones to myocytes.

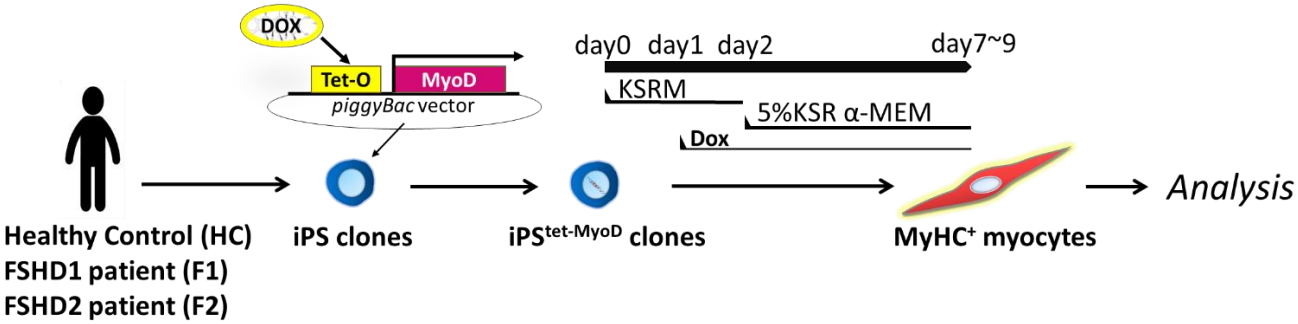

Figure 3. iPS$^{tet\text{-}MyoD}$ clones were generated from a healthy control, FSHD1 and FSHD2 patients.

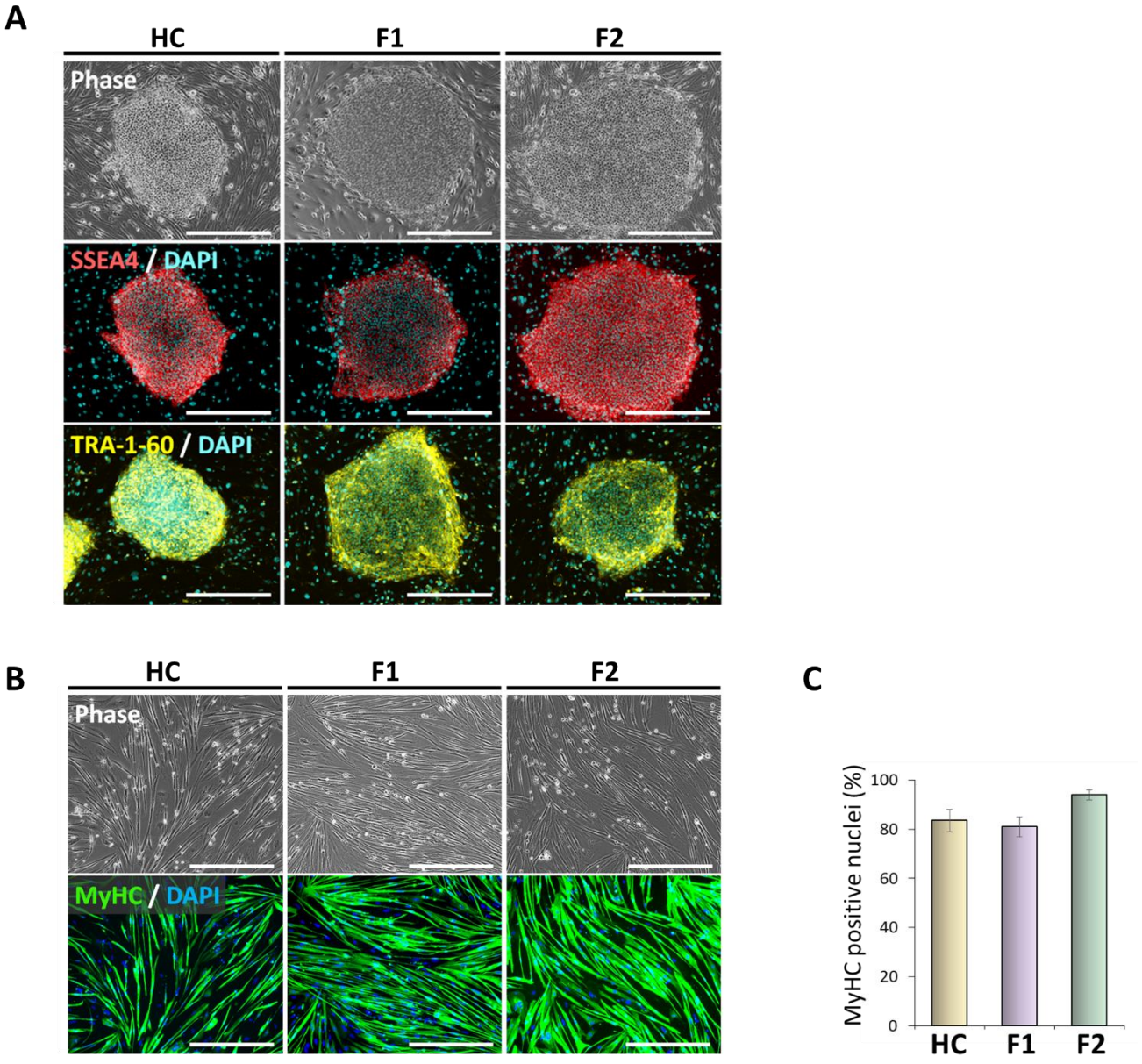

A) Immunostaining of undifferentiated iPSC$^{tet\text{-}MyoD}$ clones against SSEA4 and TRA-1-60.

B) Immunostaining of differentiated myocytes at Day 8 against myosin heavy chain (MyHC).

C) Differentiation efficiency is calculated by the percentage of MyHC positive nuclei at Day 8 (n=4).

Scale bar, 500 µm. All data are represented as mean ± SEM.

Figure 4. Gene expression analysis showed efficient myogenic differentiation and disease- and myocyte-specific *DUX4* expression.

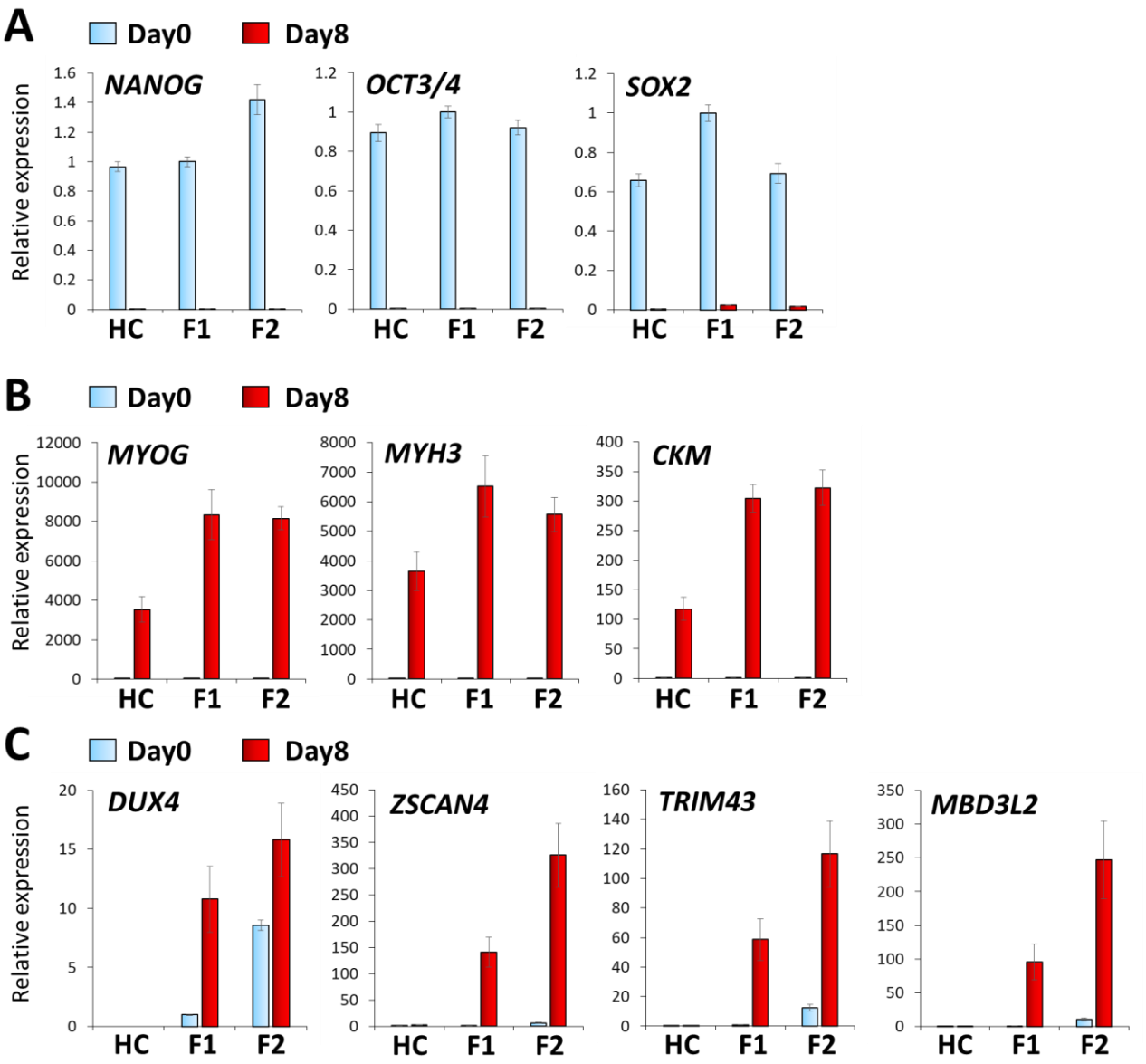

RT-qPCR analysis among Day 0 (undifferentiated) and Day 8 (differentiated) of each clone A) pluripotency markers, B) myogenic markers and C) *DUX4* and its downstream targets (n=3) . Relative expression was normalized to F1 at Day 0.

All data are represented as mean ± SEM.

Figure 5. DNA methylation of D4Z4 region was stably low in F1 (FSHD1) clone independently reprogramming or differentiation.

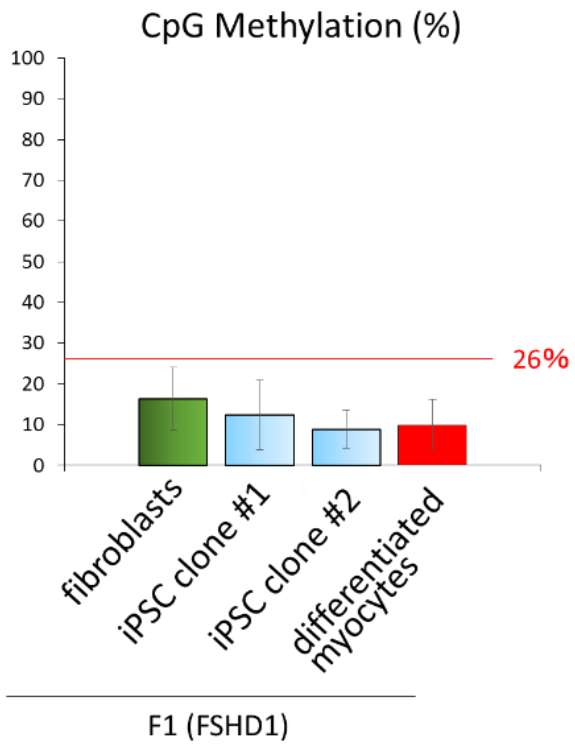

All data are represented as mean ± SEM.

Figure 6. Oxidative stress increased *DUX4* expression in FSHD myocytes.

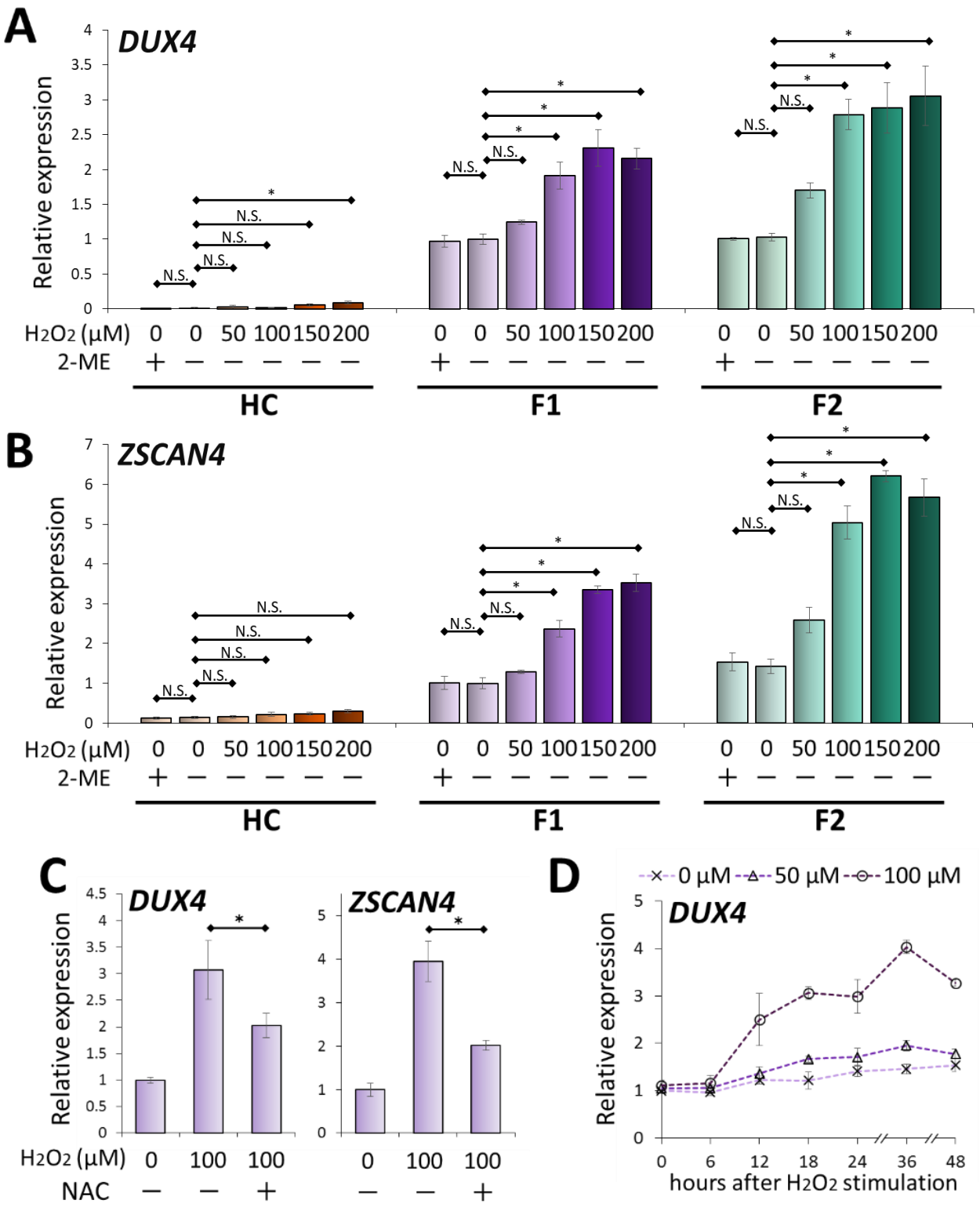

A-B) Myocytes at Day 8 were stimulated by H_2O_2 at varieties of concentration for 24 hours and RT-qPCR was performed for *DUX4* (A) and *ZSCAN4* (B). Relative expression was normalized to F1 without H_2O_2. *$P \leq 0.05$, N.S. not significant (One way ANOVA followed by Dunnett's Multiple Comparison Test).

C) NAC was pretreated one hour before H_2O_2 stimulation to F1 myocytes at Day 8 and after 24 hours RT-qPCR was performed for *DUX4* and *ZSCAN4*. Relative expression was normalized to the condition without H_2O_2 nor NAC. *$p < 0.05$ (Student's t test).

D) Time course analysis of *DUX4* mRNA expression by RT-qPCR after H_2O_2 stimulation (n=3 per each time point). Relative expression was normalized to the condition with 0 μM H_2O_2.

All data are represented as mean ± SEM.

Figure 7. Representative images of myocytes of each clone at varieties of H_2O_2 concentration.

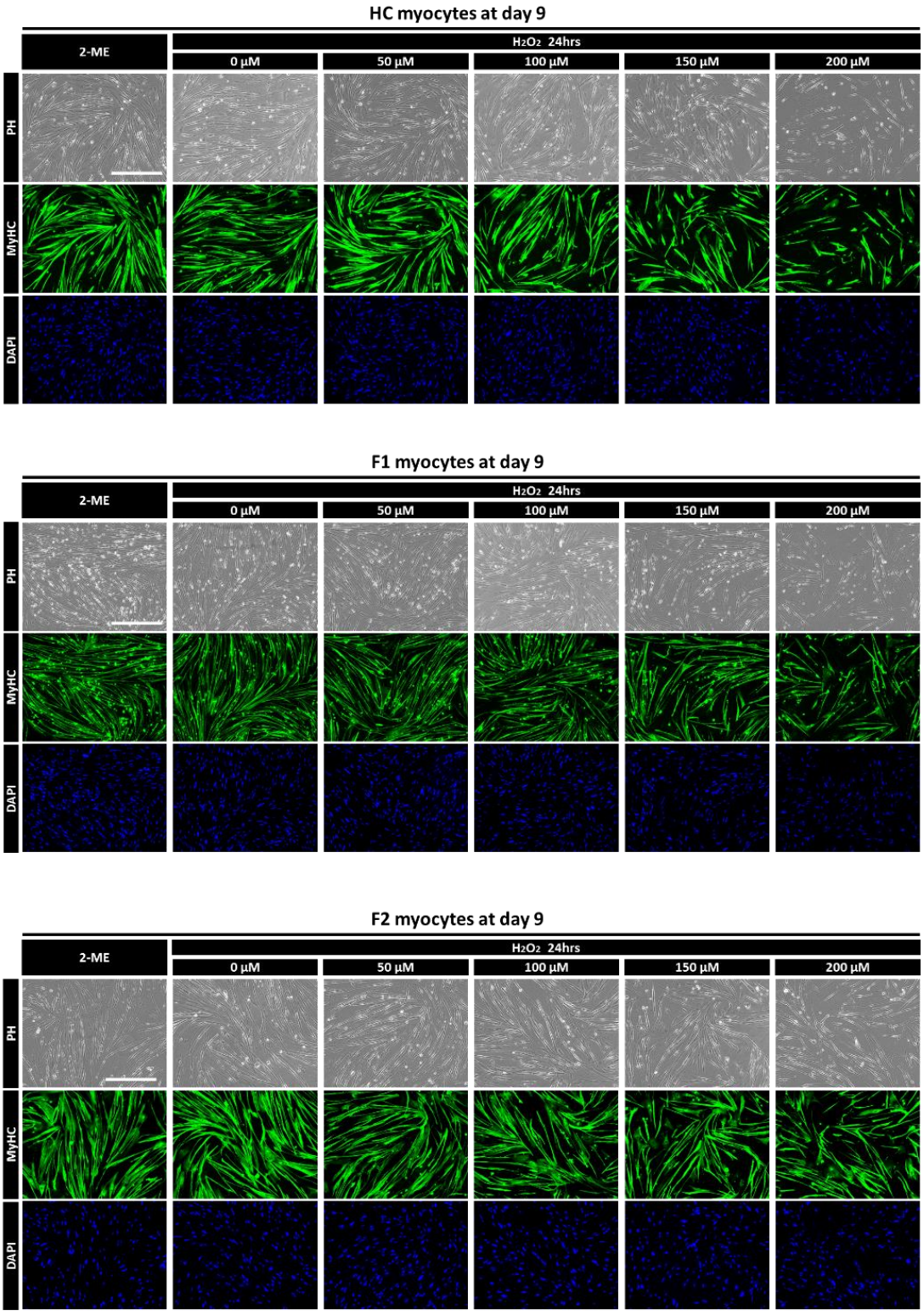

Scale bar: 500 μm

Figure 8. F1 fibroblasts did not express *DUX4*.

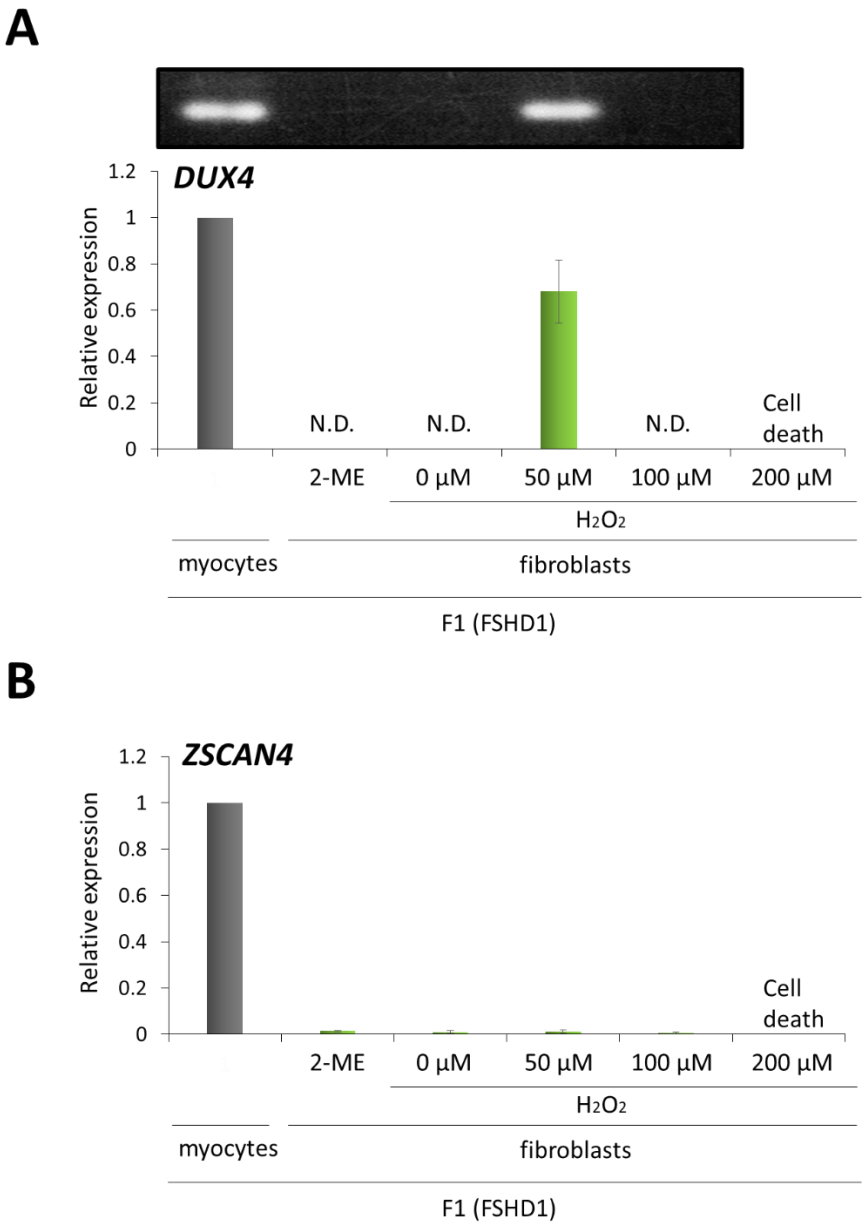

RT-qPCR analysis was performed for *DUX4* (A) and *ZSCAN4* (B) (n=3). N.D.: not detected.

The representative result of electrophoresis of the PCR-products in RT-qPCR analysis for *DUX4* is shown above the graph in (A). Note that FSHD1 fibroblasts expressed *DUX4* transcripts exclusively at 50 μM H2O2, but not downstream *ZSCAN4* at any condition.

Figure 9. Scheme of gene correction of *SMCHD1* mutation in F2 iPS$^{tet\text{-}MyoD}$ clone.

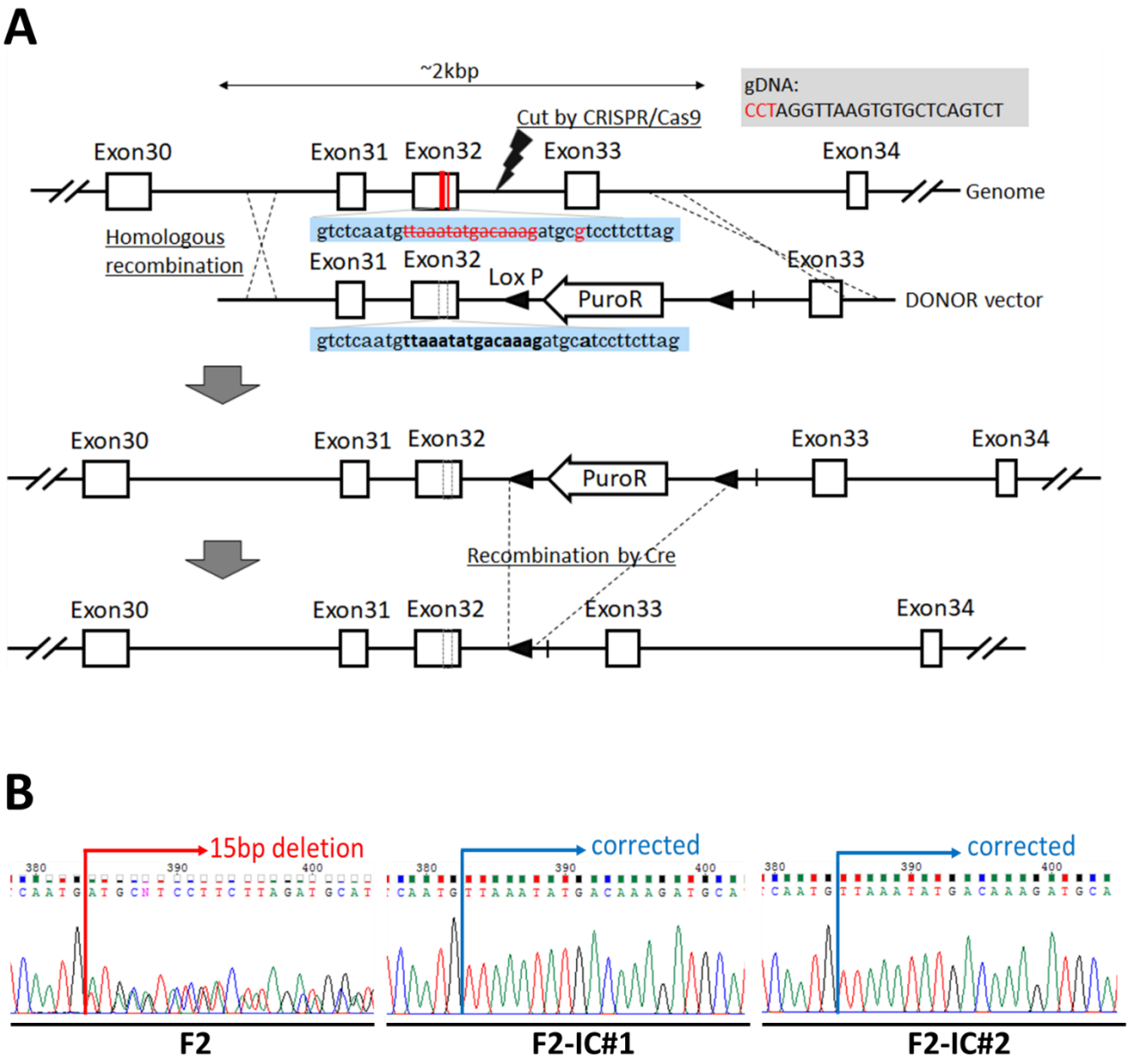

A) Scheme of gene correction of SMCHD1 mutation in F2 clone.

B) Sequence around the mutation site was checked. F2 clone has heterozygous 15 bp deletion followed by one point mutation, resulting in a ambiguous pattern of signal, but genetically-modified IC#1 and IC#2 clone show single pattern, confirming the right correction.

Figure 10. Gene-corrected F2 isogenic control iPS$^{tet\text{-}MyoD}$ clones show comparative stem cell states and efficiency of myogenic differentiation.

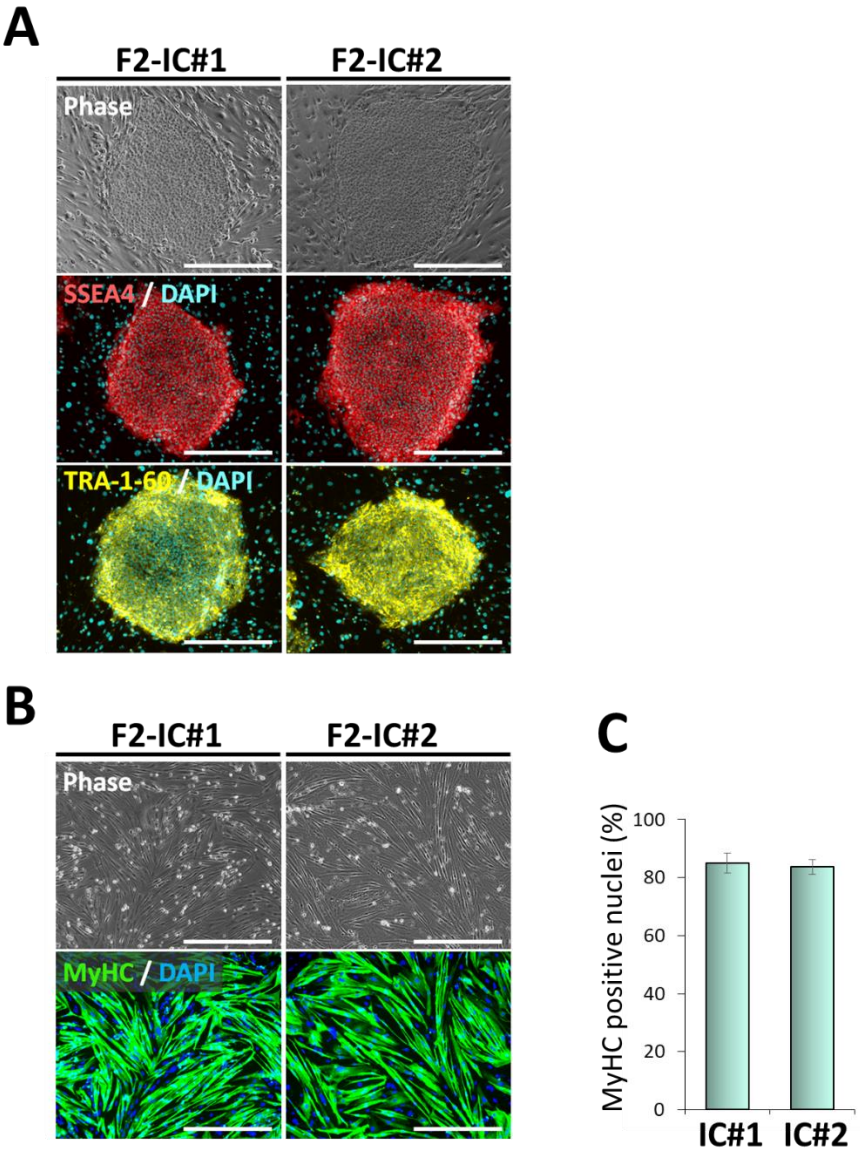

A) Immunostaining of undifferentiated iPSC$^{tet\text{-}MyoD}$ clones against SSEA4 and TRA-1-60. Refer to the parental F2 clone in Figure 3A as a control, where data were obtained at the same time as this experiment.

B) Immunostaining of differentiated myocytes at Day 8 against myosin heavy chain (MyHC). Refer to the parental F2 clone in Figure 3B as a control, where data were obtained at the same time as this experiment.

C) Differentiation efficiency is calculated by the percentage of MyHC positive nuclei at Day 8 (n=4). Refer to the parental F2 clone in Figure 3C as a control, where data were obtained at the same time as this experiment. Scale bar, 500 μm. All data are represented as mean ± SEM.

Figure 11. Gene expression analysis showed efficient myogenic differentiation and disease-specific *DUX4* expression.

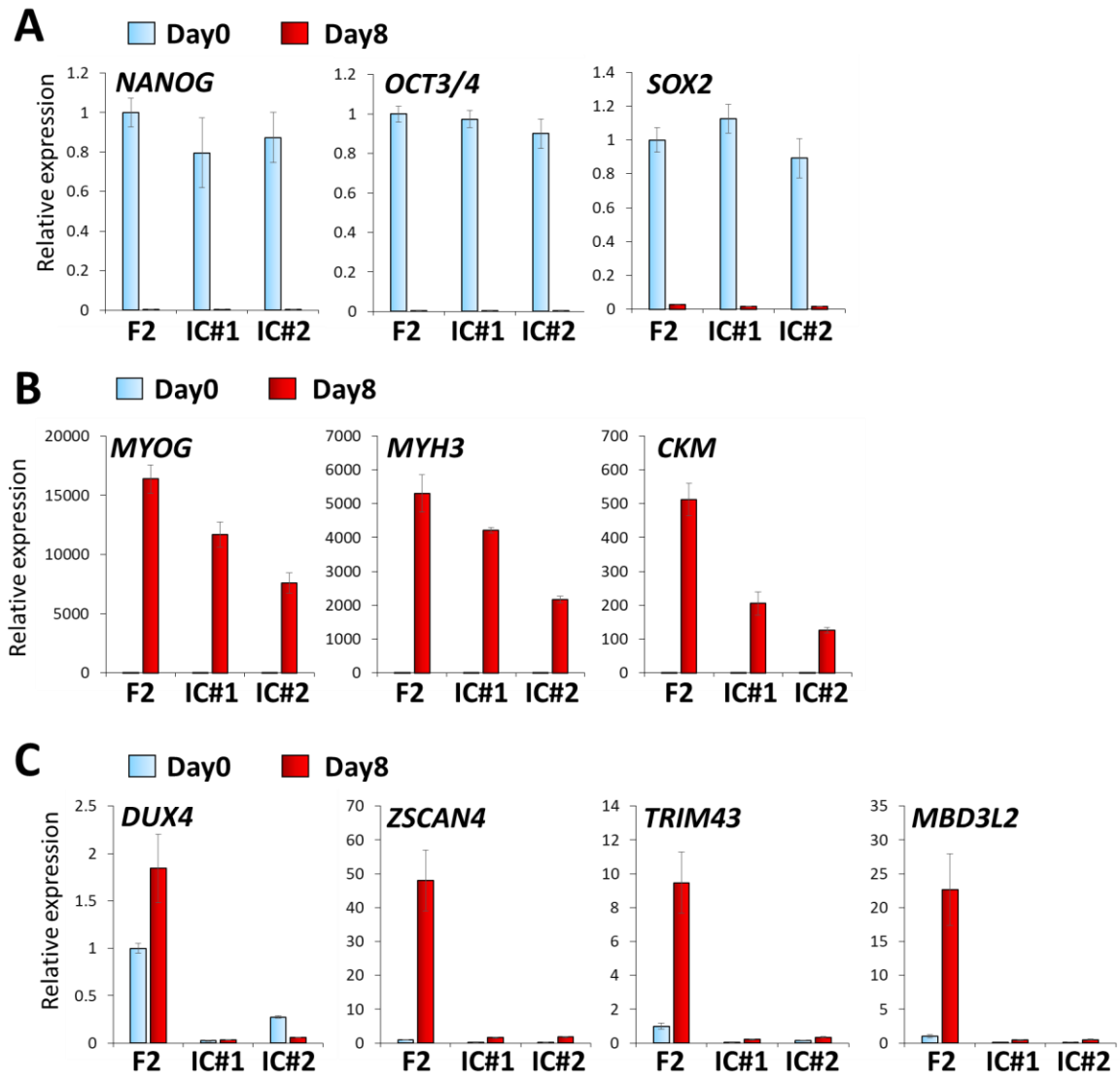

.

RT-qPCR analysis among Day 0 (undifferentiated) and Day 8 (differentiated) of each clone for pluripotency markers (A), myogenic markers (B) and *DUX4* and its downstream targets (C). Relative expression was normalized to F2 at Day 0 (n=3). All data are represented as mean ± SEM.

Figure 12. OS-induced DUX4 upregulation was suppressed by gene correction of *SMCHD1* mutation in F2 clone.

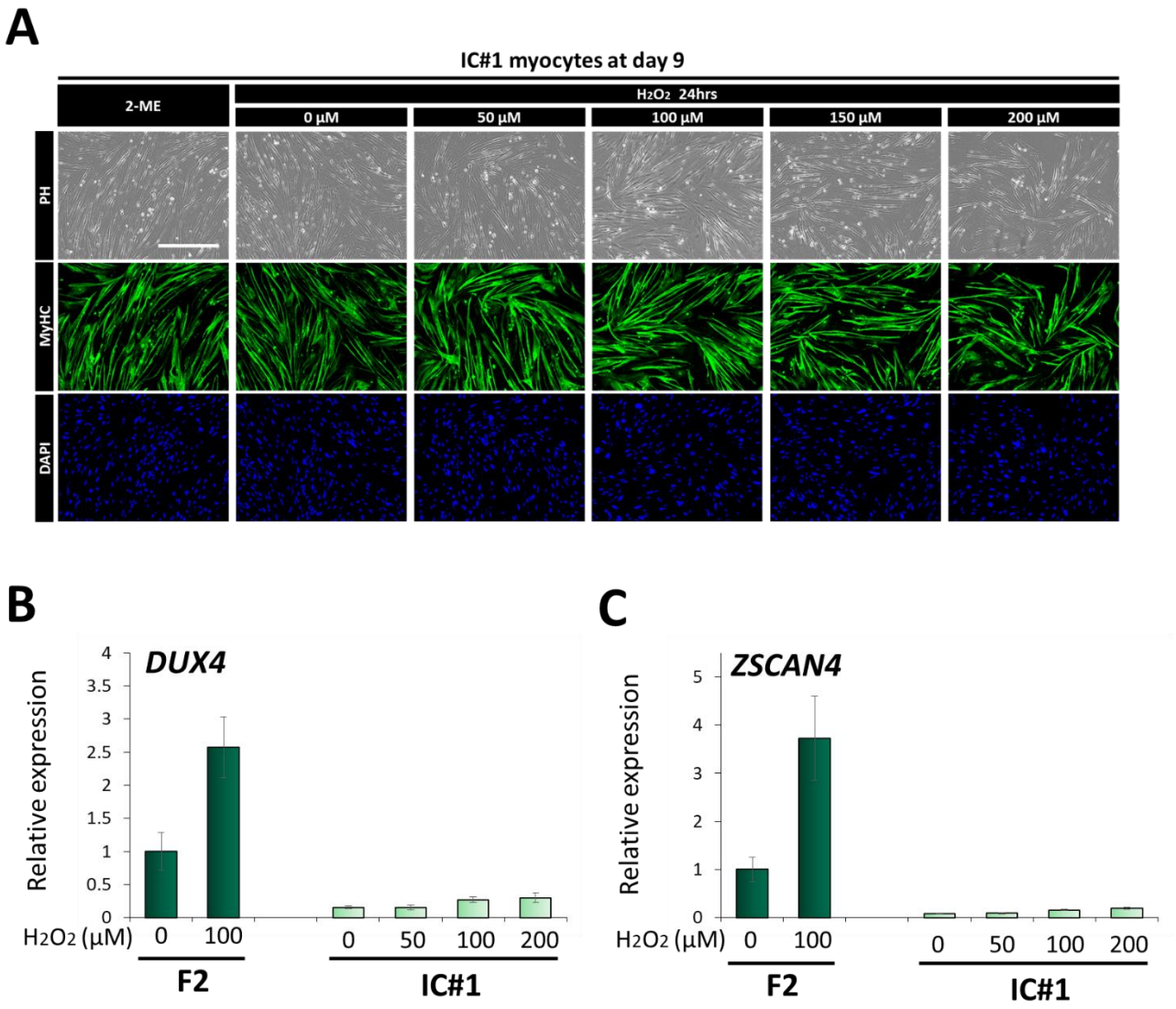

A) Representative images of myocytes of IC#1 clone at varieties of H_2O_2 concentration. Scale bar: 500 μm

B-C) RT-qPCR analysis for *DUX4* (B) and *ZSCAN4* (C) in F2 and IC#1 clone under H_2O_2 simulation. Relative expression was normalized to F2 without H_2O_2 (n=3).

Scale bar, 500 μm. All data are represented as mean ± SEM.

Figure 13. Another gene-corrected clone IC#2 also showed suppressed OS-induced *DUX4* upregulation.

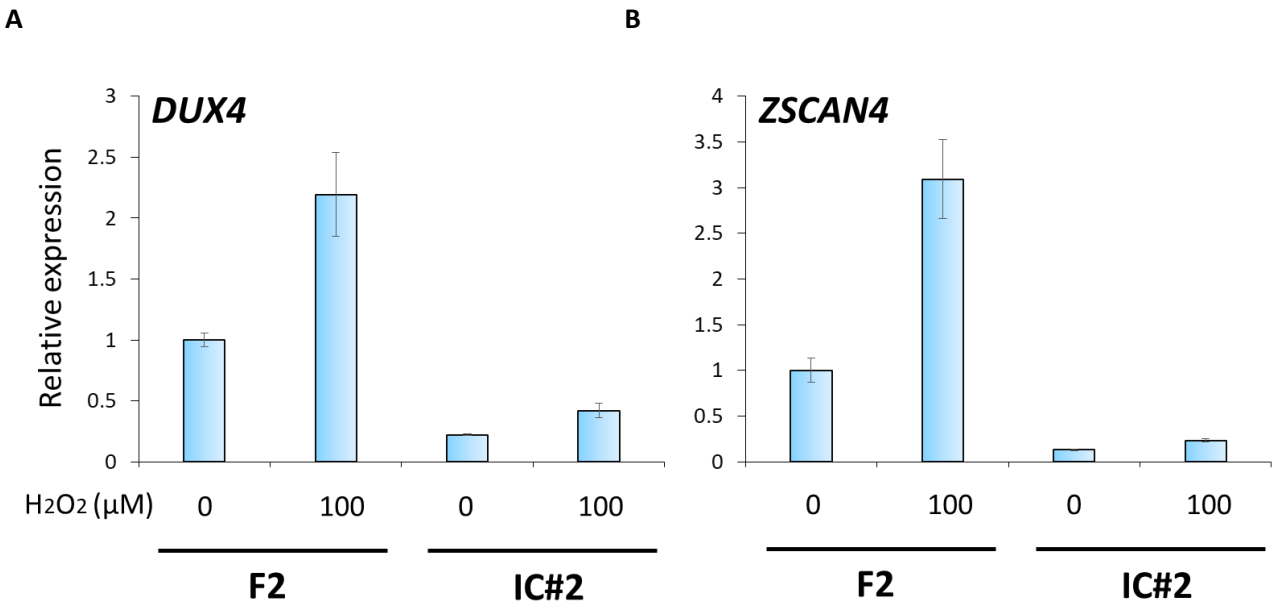

RT-qPCR analysis for *DUX4* (A) and *ZSCAN4* (B) in F2 and IC#2 myocytes under H2O2 stimulation for 24 hours.

All data are represented as mean ± SEM.

Figure 14. The 4q35 genome in FSHD2 isogenic control myocytes showed more heterochromatic state in a protein level.

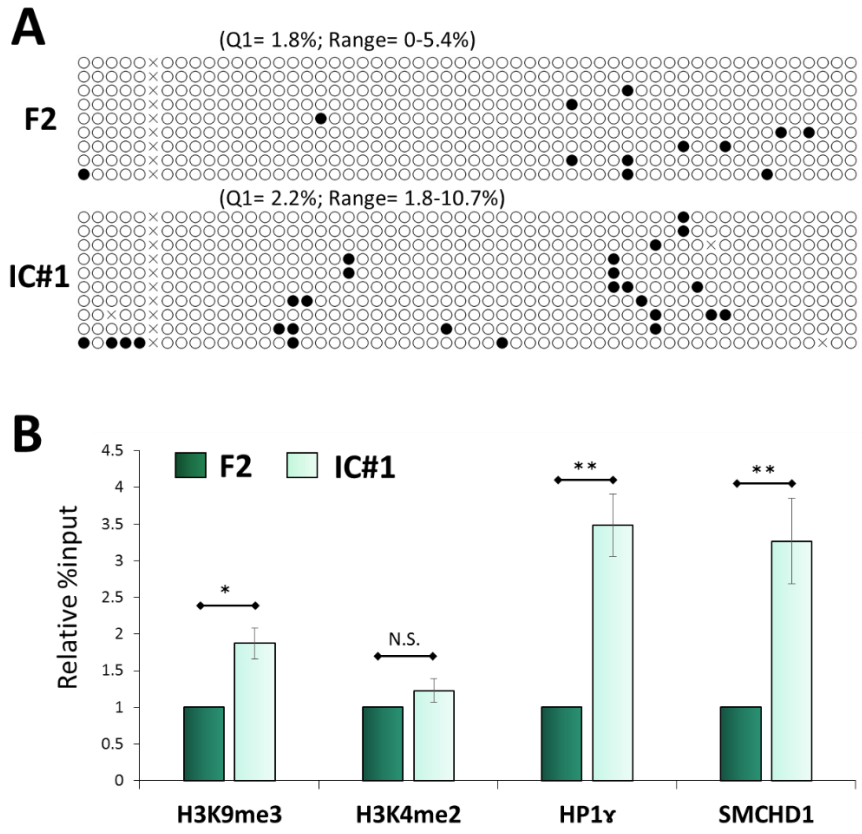

A) DNA methylation analysis on 4q35 region by bisulfite sequencing. White and black circle are unmethylated and methylated CpG, respectively. The lower quartile (Q1) and range of the percent methylation are shown above each column.

B) ChIP RT-qPCR was performed on 4q35 by H3K9me3, H3K4me2 (as a negative control), HP1γ and SMCHD1 (n=4). Relative %input was normalized to F2.

All data are represented as mean ± SEM. *p < 0.05, **p < 0.01 (Student's t test).

Figure 15. IC#2 also showed similar *DUX4* expression and epigenetic features as IC#1.

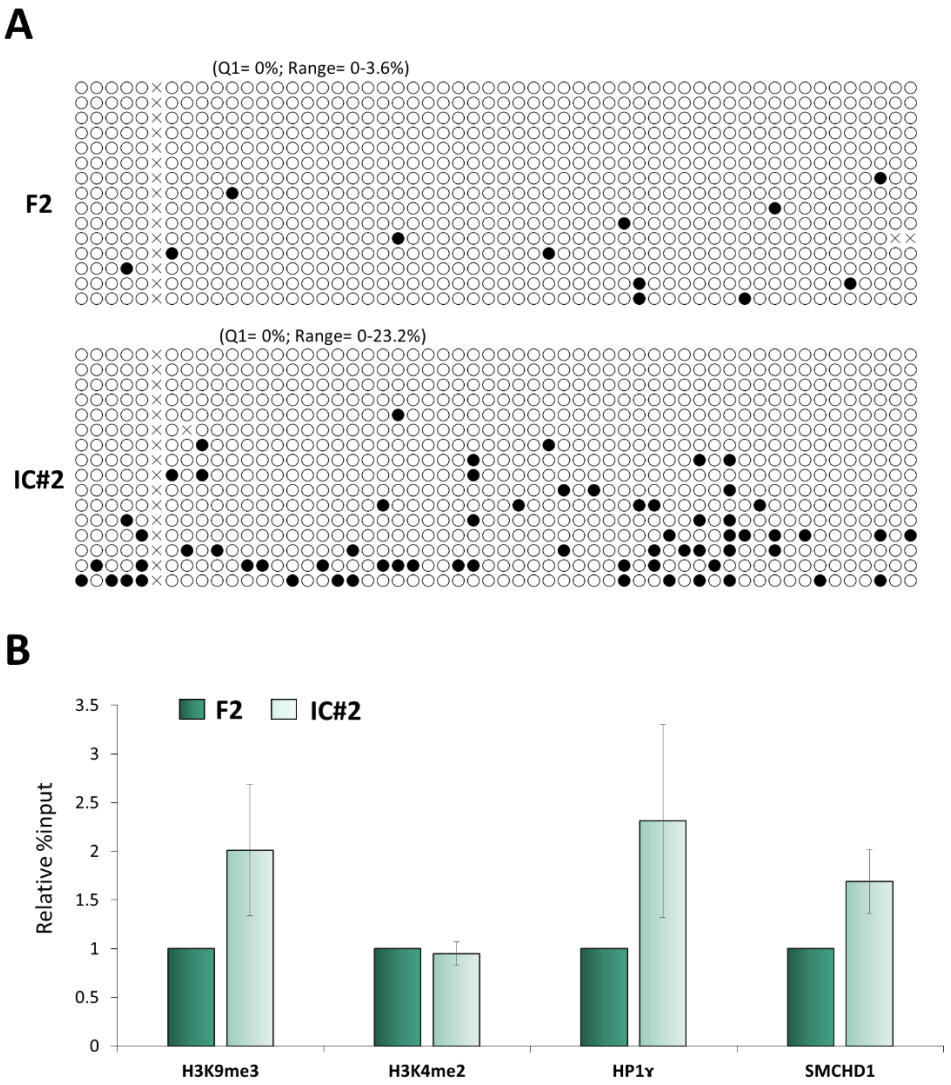

A) DNA methylation analysis on 4q35.

B) ChIP RT-qPCR was performed on 4q35 by H3K9me3, H3K4me2 (as a negative control), HP1γ and SMCHD1 (n=2). Relative %input was normalized to F2.

Figure 16. LncRNA DBE-T expression was correlated with *DUX4* expression.

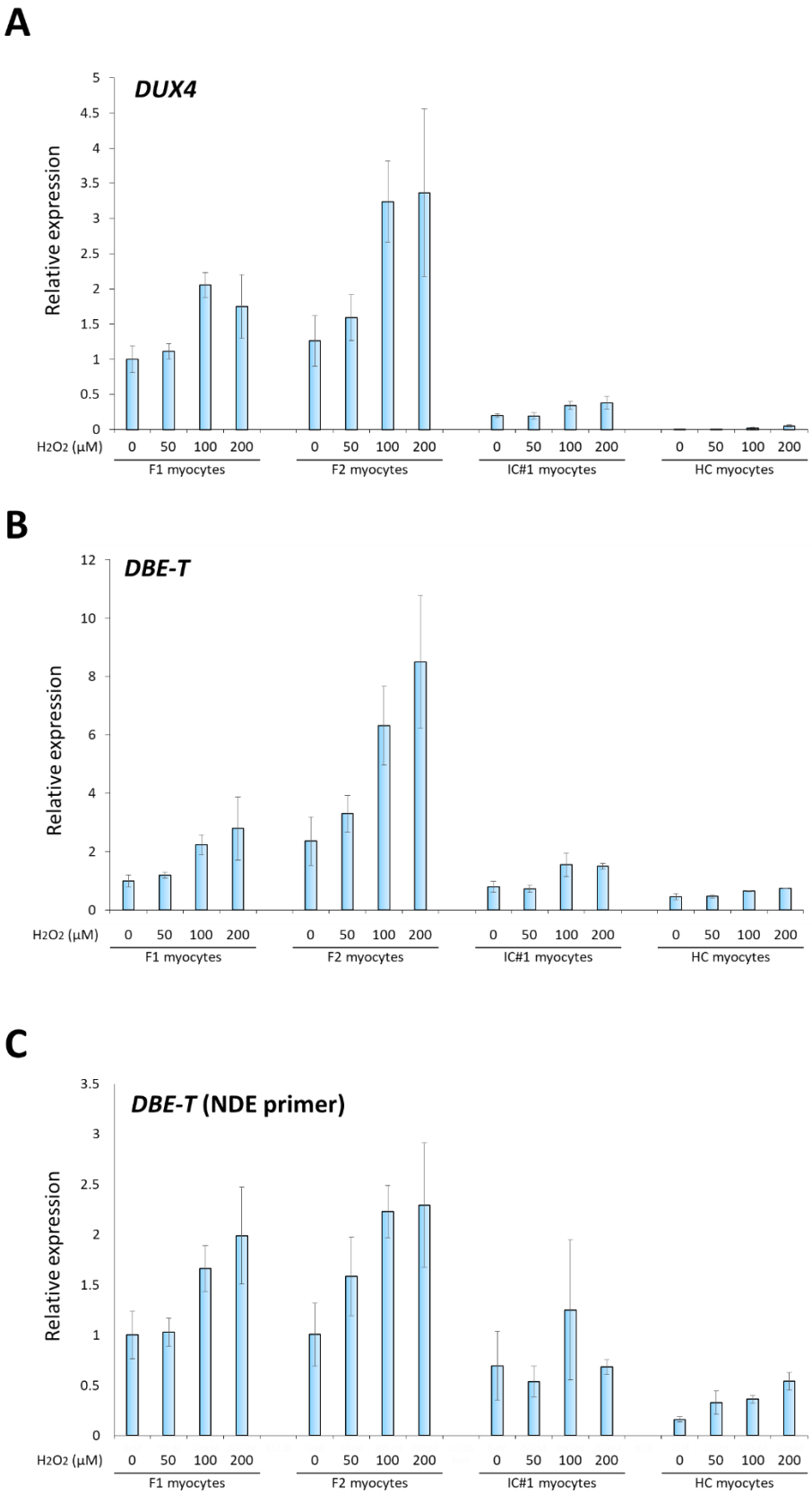

RT-qPCR analysis for *DUX4* (A), *DBE-T* (B), and *DBE-T* by another set of primers (C) among myocytes of each clone at varieties of H_2O_2 concentration (n=3).

Figure 17. Knockdown experiments of DBE-T in F1 myocytes by shRNA (short-hairpin RNA).

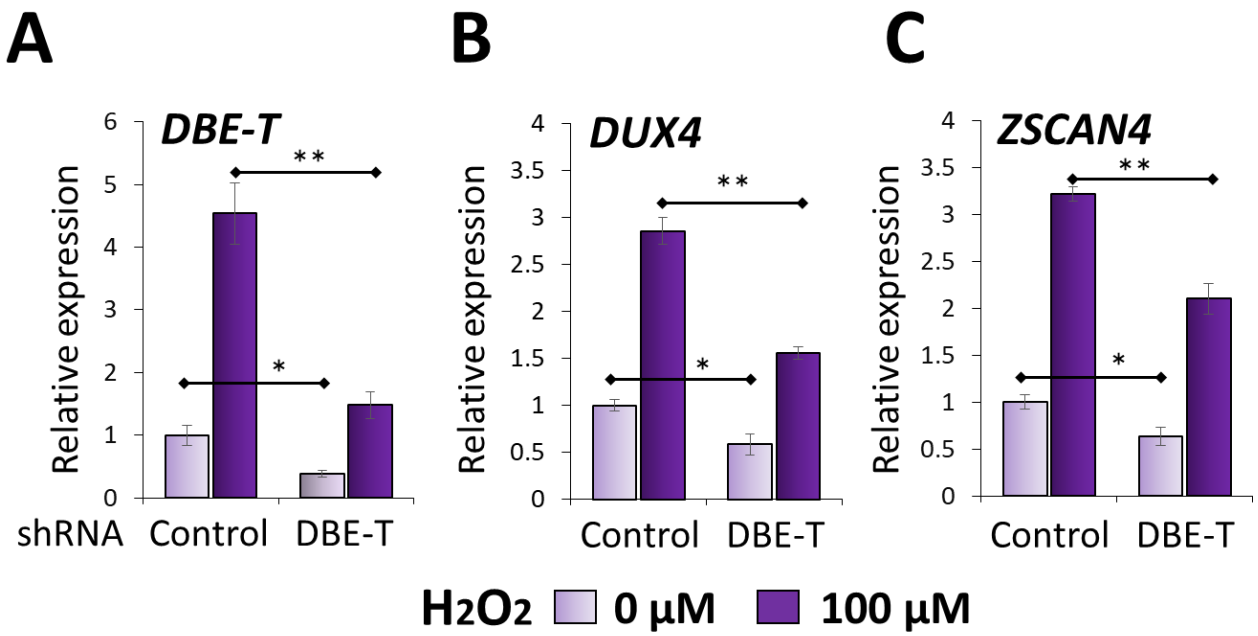

RT-qPCR analysis was performed for *DBE-T* (A), *DUX4* (B) and *ZSCAN4* (C) (n=3).

All data are represented as mean ± SEM. *p < 0.05, **p < 0.01 (Student's t test).

Figure 18. DNA damage response followed H_2O_2 stimulation.

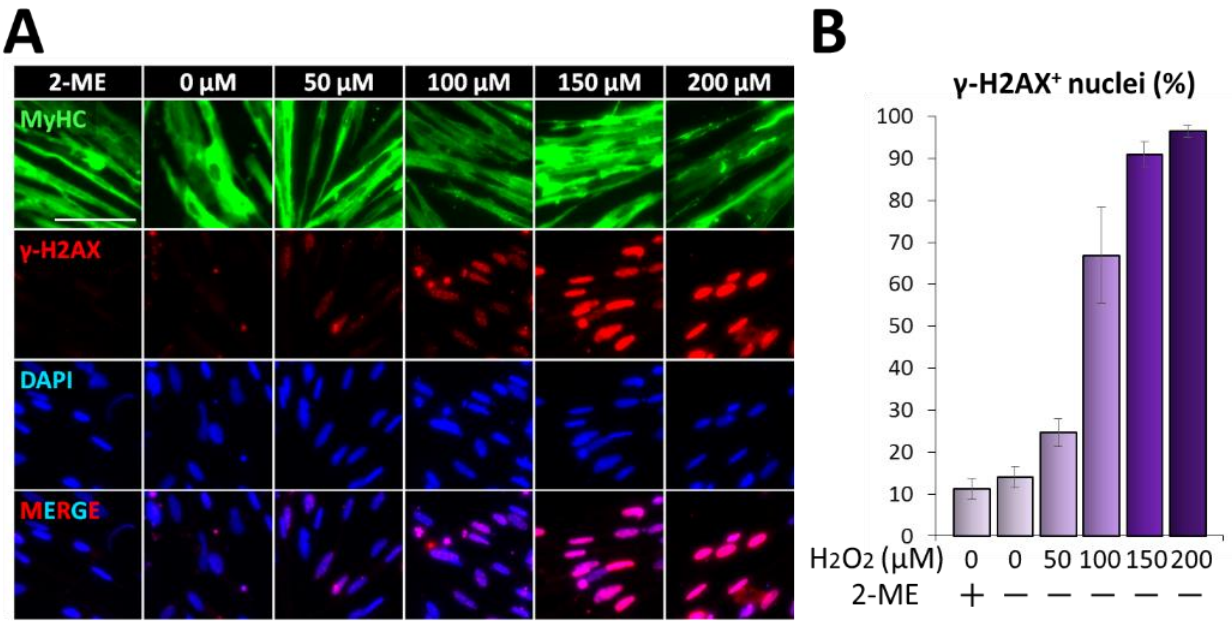

A) Representative images of Immunostaining of MyHC (green), γ-H2AX (red) and nuclei (blue) of F1 myocytes in the absence or presence of H_2O_2 stimulation.

B) The percentage of γ-H2AX positive nuclei in A) (n=3).

Scale bar, 100 µm. All data are represented as mean ± SEM.

Figure 19. UV-C exposure increased *DUX4* expression in F1 myocytes.

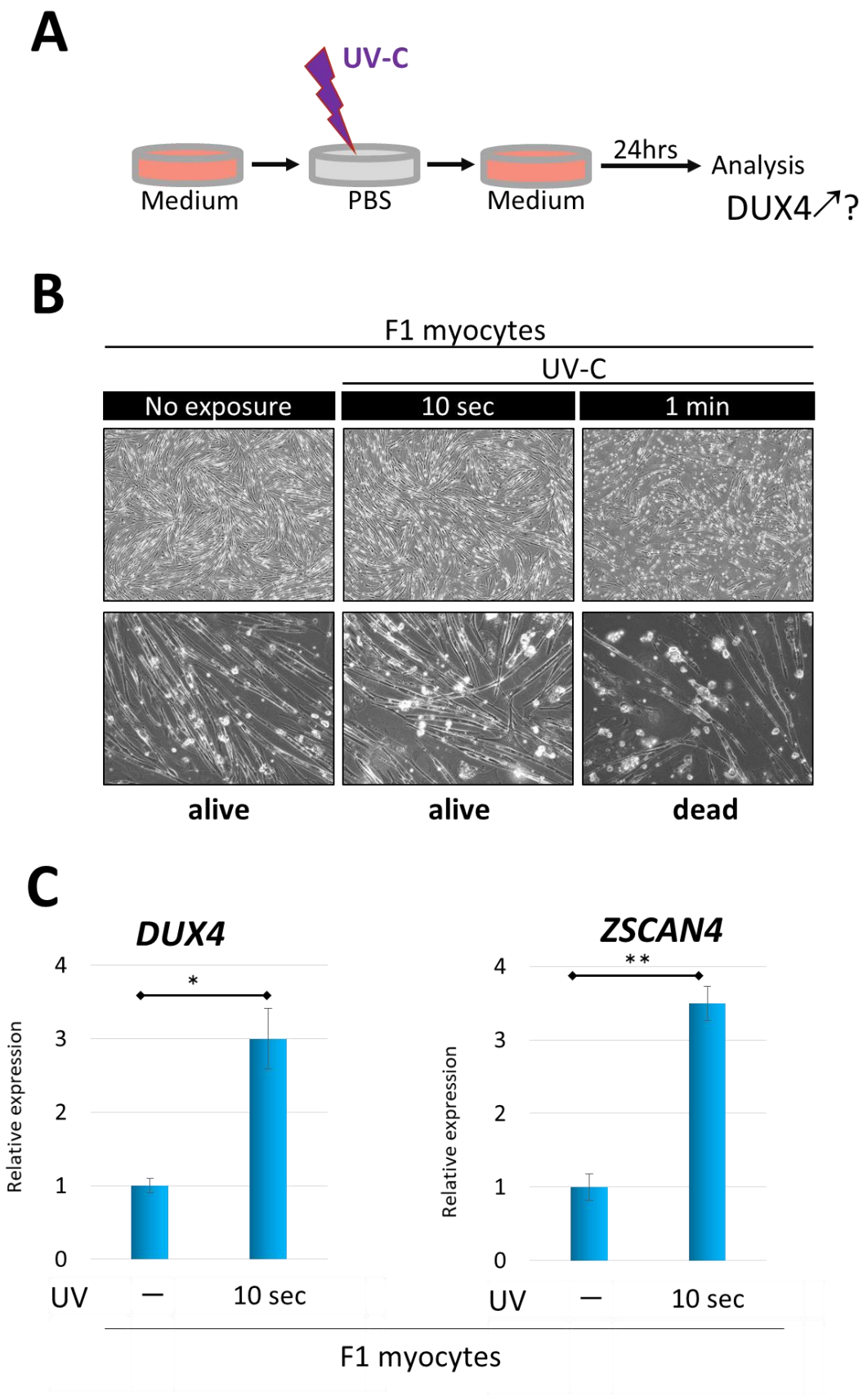

A) Scheme of UV-C exposure. UV-C in the laminar flow cabinet was used. The estimated power is ~1 J・m^{-2}・s^{-1}.

B) Representative images of myocytes exposed to UV-C. 10 seconds, but not 1 min of UV-C to F1 myocytes allowed cell survival.

C) RT-qPCR analysis for *DUX4* and *ZSCAN4* in (B) (n=3).

All data are represented as mean ± SEM.

Figure 20. Mitomycin C exposure increased *DUX4* expression in F1 myocytes.

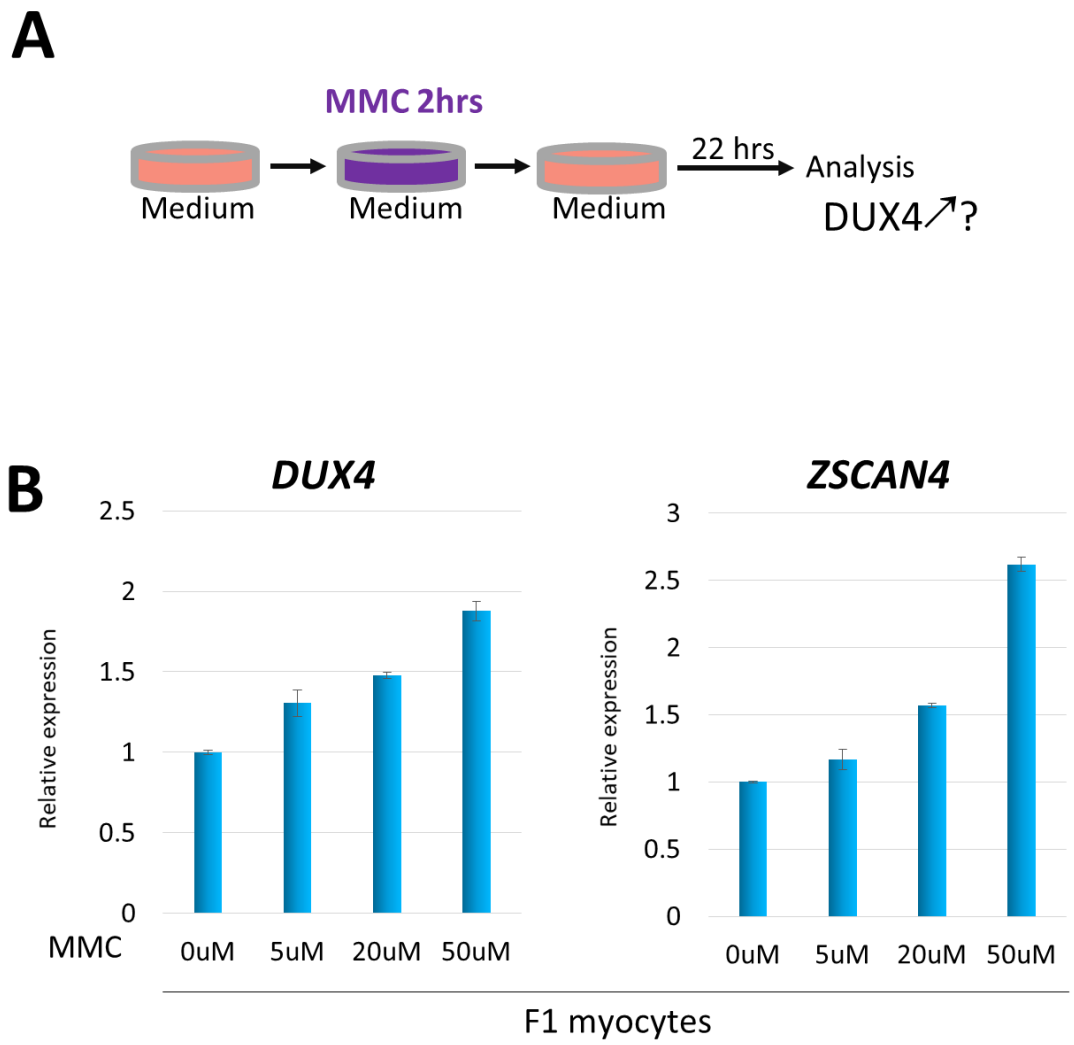

A) Scheme of DNA damage inducing by Mitomycin C (MMC) in F1 myocytes (n=3).

B) RT-qPCR analysis for *DUX4* and *ZSCAN4* in (A) (n=3).

Figure 21. ATM inhibition suppressed *DUX4* increase by OS.

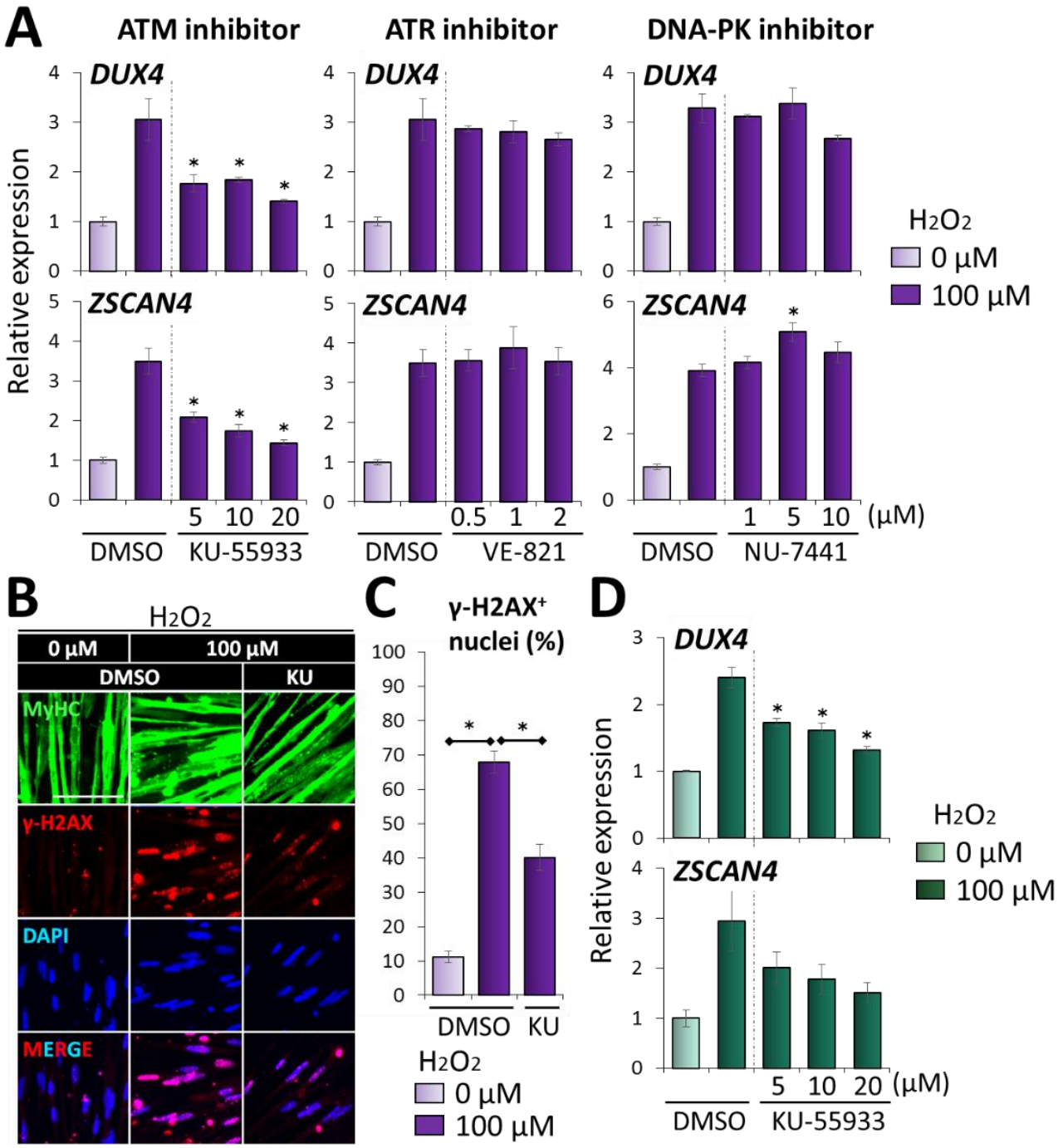

A) *DUX4* and *ZSCAN4* mRNA expression in F1 myocytes under H_2O_2 stimulation with KU-55933, VE-821 or NU-7441 (inhibitors for ATM, ATR and DNA-PK, respectively) (n=3). Relative expression was normalized to 0 µM H_2O_2. Samples were analyzed by One way ANOVA followed by Dunnett's Multiple Comparison Test. *p

< 0.05.

B) Representative images of Immunostaining of MyHC (green), γ-H2AX (red) and nuclei (blue) of F1 myocytes with or without H_2O_2 stimulation and 20 μM KU-55933. Scale bar, 100 μm.

C) The percentage of γ-H2AX positive nuclei in B) (n=4). Samples were analyzed by One way ANOVA followed by Dunnett's Multiple Comparison Test. *p < 0.05.

D) *DUX4* and *ZSCAN4* mRNA expression in F2 myocytes under H_2O_2 stimulation with KU-55933. Samples were analyzed by One way ANOVA followed by Dunnett's Multiple Comparison Test. *p < 0.05.

All data are represented as mean ± SEM.

Figure 22. Inhibition of MAPK family did not suppress *DUX4* increase by H_2O_2

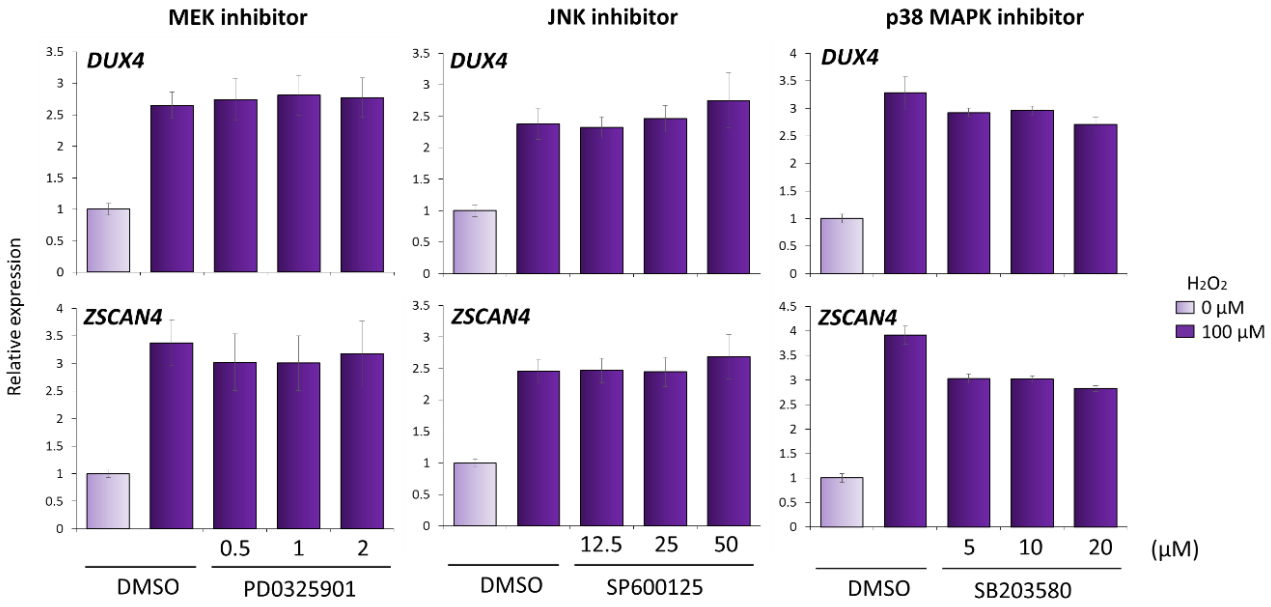

DUX4 and *ZSCAN4* mRNA expression in F1 myocytes under H_2O_2 stimulation with PD0325901, SP600125 or SB203580 (inhibitors for MEK, JNK and p38 MAPK, respectively) (n=3). Relative expression was normalized to 0 µM H_2O_2. All data are represented as mean ± SEM.

Figure 23. My model of involvement of oxidative stress in FSHD pathogenesis.

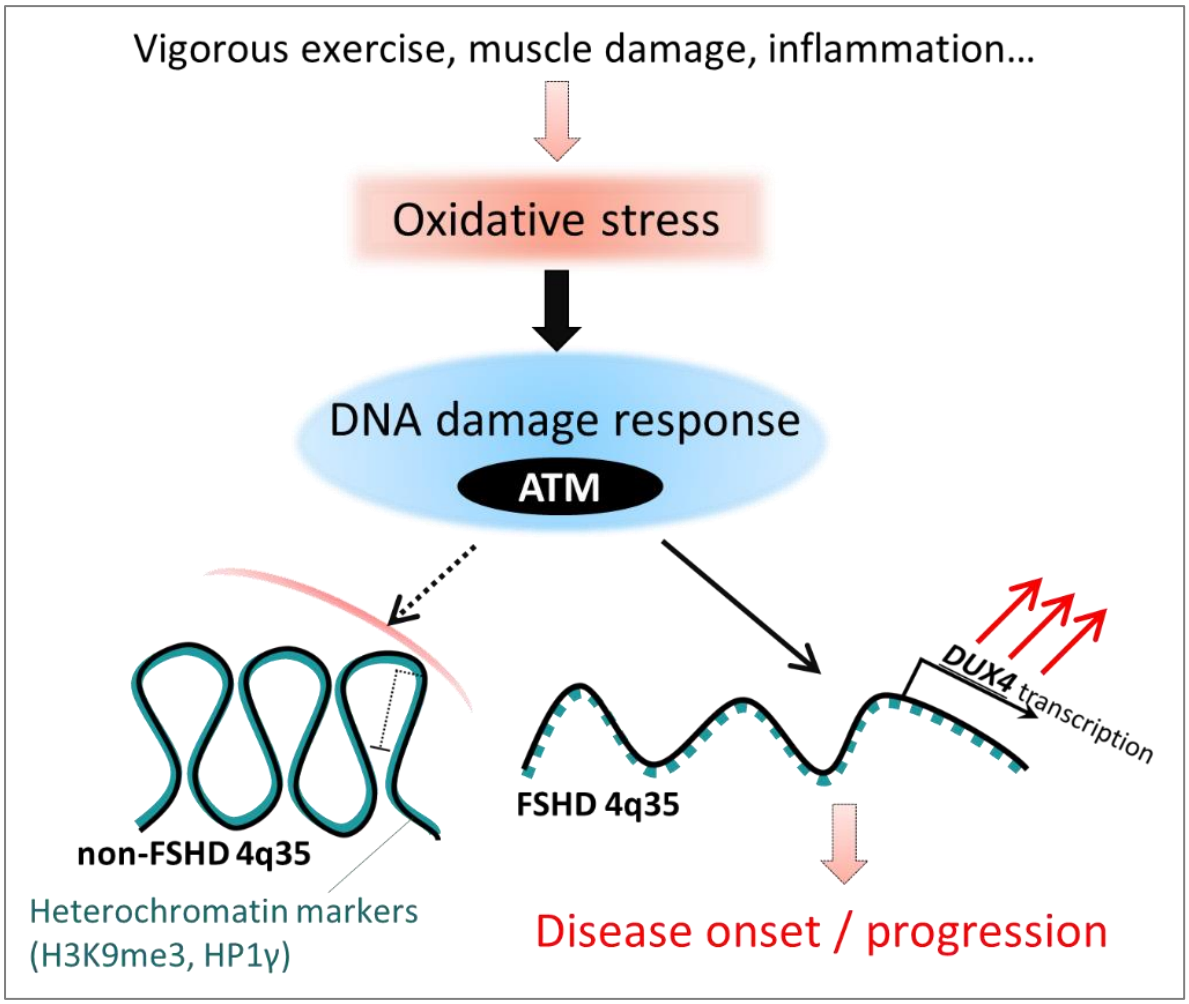

Oxidative stress (OS) is an environmental stress which is easy to be triggered by physiological conditions such as extreme exercise, muscle damage or inflammation in skeletal muscle. OS causes transient DNA damage response mediated by ATM signaling, which is kept away from non-FSHD "closed" 4q35 chromatin, but has an aberrant access to FSHD "opened" 4q35 chromatin. This causes up-regulation of *DUX4* gene expression and can affect disease onset or progression.

7. REFERENCES

1. Upadhhyaya,M. and Cooper,D. (2004) Facioscapulohumeral Muscular Dystrophy (FSHD): Clinical Medicine and Molecular Cell Biology. *Garland Science*.

2. Tawil,R., van der Maarel,S.M. and Tapscott,S.J. (2014) Facioscapulohumeral dystrophy: the path to consensus on pathophysiology. *Skelet. Muscle*, **4**, 12.

3. Daxinger,L., Tapscott,S.J. and van der Maarel,S.M. (2015) Genetic and epigenetic contributors to FSHD. *Curr. Opin. Genet. Dev.*, **33**, 56–61.

4. Lemmers,R.J.L.F., Vliet,P.J. Van Der, Klooster,R., Sacconi,S., Dauwerse,J.G., Snider,L., Straasheijm,K.R., Van,G.J., Padberg,G.W., Miller,D.G., *et al.* (2010) A unifying genetic model for facioscapulohumeral muscular dystrophy. *Science (80-.).*, **329**, 1650–1653.

5. Zeng,W., De Greef,J.C., Chen,Y.Y., Chien,R., Kong,X., Gregson,H.C., Winokur,S.T., Pyle,A., Robertson,K.D., Schmiesing,J.A., *et al.* (2009) Specific loss of histone H3 lysine 9 trimethylation and HP1γ/cohesin binding at D4Z4 repeats is associated with facioscapulohumeral dystrophy (FSHD). *PLoS Genet.*, **5**.

6. Lemmers,R.J.L.F., Goeman,J.J., Van der Vliet,P.J., Van Nieuwenhuizen,M.P., Balog,J., Vos-Versteeg,M., Camano,P., Ramos Arroyo,M.A., Jerico,I., Rogers,M.T., *et al.* (2015) Inter-individual differences in CpG methylation at D4Z4 correlate with clinical variability in FSHD1 and FSHD2. *Hum. Mol. Genet.*, **24**, 659–669.

7. Lemmers,R.J.L.F., Tawil,R., Petek,L.M., Balog,J., Block,G.J., Santen,G.W.E., Amell,A.M., Van Der

Vliet,P.J., Almomani,R., Straasheijm,K.R., *et al.* (2012) Digenic inheritance of an SMCHD1 mutation and an FSHD-permissive D4Z4 allele causes facioscapulohumeral muscular dystrophy type 2. *Nat. Genet.*, **44**, 1370–1374.

8. Geng,L.N., Yao,Z., Snider,L., Fong,A.P., Cech,J.N., Young,J.M., vanderMaarel,S.M., Ruzzo,W.L., Gentleman,R.C., Tawil,R., *et al.* (2012) DUX4 Activates Germline Genes, Retroelements, and Immune Mediators: Implications for Facioscapulohumeral Dystrophy. *Dev. Cell*, **22**, 38–51.

9. Shadle,S.C., Zhong,J.W., Campbell,A.E., Conerly,M.L., Jagannathan,S., Wong,C.J., Morello,T.D., van der Maarel,S.M. and Tapscott,S.J. (2017) DUX4-induced dsRNA and MYC mRNA stabilization activate apoptotic pathways in human cell models of facioscapulohumeral dystrophy. *PLoS Genet.*, **13**, 1–25.

10. Whiddon,J.L., Langford,A.T., Wong,C.-J., Zhong,J.W. and Tapscott,S.J. (2017) Conservation and innovation in the DUX4-family gene network. *Nat. Genet.*, **49**, 935–940.

11. De Greef,J.C., Lemmers,R.J.L.F., Camaño,P., Day,J.W., Sacconi,S., Dunand,M., Van Engelen,B.G.M., Kiuru-Enari,S., Padberg,G.W., Rosa,A.L., *et al.* (2010) Clinical features of facioscapulohumeral muscular dystrophy 2. *Neurology*, **75**, 1548–1554.

12. Ricci,E., Galluzzi,G., Deidda,G., Cacurri,S., Colantoni,L., Merico,B., Piazzo,N., Servidei,S., Vigneti,E., Pasceri,V., *et al.* (1999) Progress in the molecular diagnosis of facioscapulohumeral muscular dystrophy and correlation between the number of KpnI repeats at the 4q35 locus and clinical phenotype. *Ann. Neurol.*, **45**, 751–757.

13. Statland,J., DonlinSmith,C., Tapscott,S., Van Der Maarel,S. and Tawil,A. (2015) Milder phenotype in

facioscapulohumeral muscular dystrophy patients with the largest residual D4Z4 fragments. *Neurology*, **84**, 2147–2151.

14. Teveroni,E., Pellegrino,M., Sacconi,S., Calandra,P., Cascino,I., Farioli-Vecchioli,S., Puma,A., Garibaldi,M., Morosetti,R., Tasca,G., *et al.* (2017) Estrogens enhance myoblast differentiation in facioscapulohumeral muscular dystrophy by antagonizing DUX4 activity. *J. Clin. Invest.*, **127**, 1531–1545.

15. Block,G.J., Narayanan,D., Amell,A.M., Petek,L.M., Davidson,K.C., Bird,T.D., Tawil,R., Moon,R.T. and Miller,D.G. (2013) Wnt/β-catenin signaling suppresses DUX4 expression and prevents apoptosis of FSHD muscle cells. *Hum. Mol. Genet.*, **22**, 4661–4672.

16. Huichalaf,C., Micheloni,S., Ferri,G., Caccia,R. and Gabellini,D. (2014) DNA methylation analysis of the macrosatellite repeat associated with FSHD muscular dystrophy at single nucleotide level. *PLoS One*, **9**, 1–24.

17. Vishakha Sharma, Sachchida Nand Pandey, Hunain Khawaja, Kristy J Brown, Yetrib Hathout, and Y.-W.C. (2016) PARP1 Differentially Interacts with Promoter region of DUX4 Gene in FSHD Myoblasts. **7**, 95–121.

18. Campbell,A.E., Oliva,J., Yates,M.P., Zhong,J.W., Shadle,S.C., Snider,L., Singh,N., Tai,S., Hiramuki,Y., Tawil,R., *et al.* (2017) BET bromodomain inhibitors and agonists of the beta-2 adrenergic receptor identified in screens for compounds that inhibit DUX4 expression in FSHD muscle cells. *Skelet. Muscle*, **7**, 16.

19. Snider,L., Geng,L.N., Lemmers,R.J.L.F., Kyba,M., Ware,C.B., Nelson,A.M., Tawil,R., Filippova,G.N., van der Maarel,S.M., Tapscott,S.J., *et al.* (2010) Facioscapulohumeral dystrophy: incomplete suppression of a retrotransposed gene. *PLoS Genet.*, **6**, e1001181.

20. Rickard,A.M., Petek,L.M. and Miller,D.G. (2015) Endogenous DUX4 expression in FSHD myotubes is sufficient to cause cell death and disrupts RNA splicing and cell migration pathways. *Hum. Mol. Genet.*, **24**, 5901–5914.

21. Caron,L., Kher,D., Lee,K.L., McKernan,R., Dumevska,B., Hidalgo,A., Li,J., Yang,H., Main,H., Ferri,G., *et al.* (2016) A Human Pluripotent Stem Cell Model of Facioscapulohumeral Muscular Dystrophy-Affected Skeletal Muscles. *Stem Cells Transl. Med.*, **5**, 1145–1161.

22. Bosnakovski,D., Chan,S.S.K., Recht,O.O., Hartweck,L.M., Gustafson,C.J., Athman,L.L., Lowe,D.A. and Kyba,M. (2017) Muscle pathology from stochastic low level DUX4 expression in an FSHD mouse model. *Nat. Commun.*, **8**, 550.

23. Mason,S. and Wadley,G.D. (2014) Skeletal muscle reactive oxygen species: A target of good cop/bad cop for exercise and disease. *Redox Rep.*, **19**, 97–106.

24. Kozakowska,M., Pietraszek-Gremplewicz,K., Jozkowicz,A. and Dulak,J. (2015) The role of oxidative stress in skeletal muscle injury and regeneration: focus on antioxidant enzymes. *J. Muscle Res. Cell Motil.*, **36**, 377–393.

25. Turki,A., Hayot,M., Carnac,G., Pillard,F., Passerieux,E., Bommart,S., De Mauverger,E.R., Hugon,G., Pincemail,J., Pietri,S., *et al.* (2012) Functional muscle impairment in facioscapulohumeral muscular

dystrophy is correlated with oxidative stress and mitochondrial dysfunction. *Free Radic. Biol. Med.*, **53**, 1068–1079.

26. Passerieux,E., Hayot,M., Jaussent,A., Carnac,G., Gouzi,F., Pillard,F., Picot,M.C., Böcker,K., Hugon,G., Pincemail,J., *et al.* (2015) Effects of vitamin C, vitamin E, zinc gluconate, and selenomethionine supplementation on muscle function and oxidative stress biomarkers in patients with facioscapulohumeral dystrophy: A double-blind randomized controlled clinical trial. *Free Radic. Biol. Med.*, **81**, 158–169.

27. Winokur,S.T., Barrett,K., Martin,J.H., Forrester,J.R., Simon,M., Tawil,R., Chung,S.A., Masny,P.S. and Figlewicz,D.A. (2003) Facioscapulohumeral muscular dystrophy (FSHD) myoblasts demonstrate increased susceptibility to oxidative stress. *Neuromuscul. Disord.*, **13**, 322–333.

28. Bou Saada,Y., Dib,C., Dmitriev,P., Hamade,A., Carnac,G., Laoudj-Chenivesse,D., Lipinski,M. and Vassetzky,Y.S. (2016) Facioscapulohumeral dystrophy myoblasts efficiently repair moderate levels of oxidative DNA damage. *Histochem. Cell Biol.*, **145**, 475–483.

29. Dmitriev,P., Bou Saada,Y., Dib,C., Ansseau,E., Barat,A., Hamade,A., Dessen,P., Robert,T., Lazar,V., Louzada,R.A.N., *et al.* (2016) DUX4-induced constitutive DNA damage and oxidative stress contribute to aberrant differentiation of myoblasts from FSHD patients. *Free Radic. Biol. Med.*, **99**, 244–258.

30. Winokur,S.T., Chen,Y.W., Masny,P.S., Martin,J.H., Ehmsen,J.T., Tapscott,S.J., van der Maarel,S.M., Hayashi,Y. and Flanigan,K.M. (2003) Expression profiling of FSHD muscle supports a defect in specific stages of myogenic differentiation. *Hum. Mol. Genet.*, **12**, 2895–2907.

31. Celegato,B., Capitanio,D., Pescatori,M., Romualdi,C., Pacchioni,B., Cagnin,S., Viganò,A., Colantoni,L., Begum,S., Ricci,E., *et al.* (2006) Parallel protein and transcript profiles of FSHD patient muscles correlate to the D4Z4 arrangement and reveal a common impairment of slow to fast fibre differentiation and a general deregulation of MyoD-dependent genes. *Proteomics*, **6**, 5303–5321.

32. Tsumagari,K., Chang,S.-C., Lacey,M., Baribault,C., Chittur,S. V, Sowden,J., Tawil,R., Crawford,G.E. and Ehrlich,M. (2011) Gene expression during normal and FSHD myogenesis. *BMC Med. Genomics*, **4**, 67.

33. Takahashi,K., Tanabe,K., Ohnuki,M., Narita,M., Ichisaka,T., Tomoda,K. and Yamanaka,S. (2007) Induction of Pluripotent Stem Cells from Adult Human Fibroblasts by Defined Factors. *Cell*, **131**, 861–872.

34. Avior,Y., Sagi,I. and Benvenisty,N. (2016) Pluripotent stem cells in disease modelling and drug discovery. *Nat. Rev. Mol. Cell Biol.*, **17**, 170–182.

35. Hamanaka,K., Goto,K., Arai,M., Nagao,K., Obuse,C., Noguchi,S., Hayashi,Y.K., Mitsuhashi,S. and Nishino,I. (2016) Clinical, muscle pathological, and genetic features of Japanese facioscapulohumeral muscular dystrophy 2 (FSHD2) patients with SMCHD1 mutations. *Neuromuscul. Disord.*, **26**, 472.

36. Tanaka,A., Woltjen,K., Miyake,K., Hotta,A., Ikeya,M., Yamamoto,T., Nishino,T., Shoji,E., Sehara-Fujisawa,A., Manabe,Y., *et al.* (2013) Efficient and Reproducible Myogenic Differentiation from Human iPS Cells: Prospects for Modeling Miyoshi Myopathy In Vitro. *PLoS One*, **8**.

37. Li,H.L., Gee,P., Ishida,K. and Hotta,A. (2016) Efficient genomic correction methods in human iPS cells using CRISPR-Cas9 system. *Methods*, **101**, 27–35.

38. Naito,Y., Hino,K., Bono,H. and Ui-Tei,K. (2015) CRISPRdirect: Software for designing CRISPR/Cas guide RNA with reduced off-target sites. *Bioinformatics*, **31**, 1120–1123.

39. Jones,T.I., Yan,C., Sapp,P.C., McKenna-Yasek,D., Kang,P.B., Quinn,C., Salameh,J.S., King,O.D. and Jones,P.L. (2014) Identifying diagnostic DNA methylation profiles for facioscapulohumeral muscular dystrophy in blood and saliva using bisulfite sequencing. *Clin. Epigenetics*, **6**, 23.

40. Kumaki,Y., Oda,M. and Okano,M. (2008) QUMA: quantification tool for methylation analysis. *Nucleic Acids Res.*, **36**, 170–175.

41. Cabianca,D.S., Casa,V., Bodega,B., Xynos,A., Ginelli,E., Tanaka,Y. and Gabellini,D. (2012) A long ncRNA links copy number variation to a polycomb/trithorax epigenetic switch in fshd muscular dystrophy. *Cell*, **149**, 819–831.

42. Bou Saada,Y., Zakharova,V., Chernyak,B., Dib,C., Carnac,G., Dokudovskaya,S. and Vassetzky,Y.S. (2017) Control of DNA integrity in skeletal muscle under physiological and pathological conditions. *Cell. Mol. Life Sci.*, **74**, 3439–3449.

43. Blackford,A.N. and Jackson,S.P. (2017) ATM, ATR, and DNA-PK: The Trinity at the Heart of the DNA Damage Response. *Mol. Cell*, **66**, 801–817.

44. Christmann,M. and Kaina,B. (2013) Transcriptional regulation of human DNA repair genes following genotoxic stress: Trigger mechanisms, inducible responses and genotoxic adaptation. *Nucleic Acids Res.*, **41**, 8403–8420.

45. Torres,M. and Forman,H.J. (2003) Redox signaling and the MAP kinase pathways. *Biofactors*, **17**, 287–

296.

46. Bosnakovski,D., Xu,Z., Gang,E.J., Galindo,C.L., Liu,M., Simsek,T., Garner,H.R., Agha-Mohammadi,S., Tassin,A., Coppée,F., *et al.* (2008) An isogenetic myoblast expression screen identifies DUX4-mediated FSHD-associated molecular pathologies. *EMBO J.*, **27**, 2766–2779.

47. Larsen,B.D., Rampalli,S., Burns,L.E., Brunette,S., Dilworth,F.J. and Megeney,L.A. (2010) Caspase 3/caspase-activated DNase promote cell differentiation by inducing DNA strand breaks. *Proc. Natl. Acad. Sci.*, **107**, 4230–4235.

48. Fischer,U., Ludwig,N., Raslan,A., Meier,C. and Meese,E. (2016) Gene amplification during myogenic differentiation. *Oncotarget*, **7**, 6864–6877.

49. Latella,L., Lukas,J., Simone,C., Lorenzo,P., Puri,P.L. and Bartek,J. (2004) Differentiation-Induced Radioresistance in Muscle Cells Differentiation-Induced Radioresistance in Muscle Cells. *Mol. Cell. Biol.*, **24**, 6350–6361.

50. Fortini,P., Ferretti,C., Pascucci,B., Narciso,L., Pajalunga,D., Puggioni,E.M.R., Castino,R., Isidoro,C., Crescenzi,M. and Dogliotti,E. (2012) DNA damage response by single-strand breaks in terminally differentiated muscle cells and the control of muscle integrity. *Cell Death Differ.*, **19**, 1741–1749.

51. Jang,E.R., Choi,J.D., Park,M.A., Jeong,G., Cho,H. and Lee,J.-S. (2010) ATM modulates transcription in response to histone deacetylase inhibition as part of its DNA damage response. *Exp. Mol. Med.*, **42**, 195–204.

52. Cowell,I.G., Sunter,N.J., Singh,P.B., Austin,C.A., Durkacz,B.W. and Tilby,M.J. (2007) γ-H2AX foci form

preferentially in euchromatin after ionising-radiation. *PLoS One*, **2**, 1–8.

53. Kim,J.A., Kruhlak,M., Dotiwala,F., Nussenzweig,A. and Haber,J.E. (2007) Heterochromatin is refractory to γ-H2AX modification in yeast and mammals. *J. Cell Biol.*, **178**, 209–218.

54. Murga,M., Jaco,I., Fan,Y., Soria,R., Martinez-Pastor,B., Cuadrado,M., Yang,S.M., Blasco,M.A., Skoultchi,A.I. and Fernandez-Capetillo,O. (2007) Global chromatin compaction limits the strength of the DNA damage response. *J. Cell Biol.*, **178**, 1101–1108.

55. Choi,S.H., Gearhart,M.D., Cui,Z., Bosnakovski,D., Kim,M., Schennum,N. and Kyba,M. (2016) DUX4 recruits p300/CBP through its C-terminus and induces global H3K27 acetylation changes. *Nucleic Acids Res.*, **44**, 5161–5173.

56. Ferreboeuf,M., Mariot,V., Bessières,B., Vasiljevic,A., Attié-Bitach,T., Collardeau,S., Morere,J., Roche,S., Magdinier,F., Robin-Ducellier,J., *et al.* (2014) DUX4 and DUX4 downstream target genes are expressed in fetal FSHD muscles. *Hum. Mol. Genet.*, **23**, 171–181.

8. ACKNOWLEDGEMENTS

8-1. FUNDING

This work was supported by a grant from the Program for Intractable Diseases Research utilizing disease-specific iPS cells, which were provided by the Japan Agency for Medical Research and Development, AMED (to H.S.); the Japan Society for the Promotion of Science KAKENHI [17J04509 to M.S.H.]; and a grant-in-aid of The Intramural Research Grant [29-4] for Neurological and Psychiatric Disorders of National Center of Neurology and Psychiatry and the Fugaku Trust for Medical Research (to R.M.).

8-2. SPECIAL THANKS

I appreciate both of my supervisors, Dr. Hidetoshi Sakurai at Center for iPS cell Research and Application (CiRA), Kyoto Univ., and Dr. Ryoichi Matsuda in the Univ. of Tokyo. Dr. Sakurai has provided an environment to proceed this research with his productive instruction and Dr. Matsuda has provided a great chance to pursue my own goal. I appreciate all the members of the laboratory of Dr. Sakurai and the laboratory of Dr. Matsuda, especially because of lots of supports for my physical handicap. I am grateful to the devoted donors for iPSCs establishment. I am grateful to Dr. Ichizo Nishino at the National Center of Neurology and Psychiatry (NCNP) and Dr. Satomi Mistuhasi at NCNP and Yokohama City Univ. for introduction of the donors and also for DNA methylation analysis as collaborators. I am grateful to Mr. Tatsuya Jonouchi at CiRA for iPSCs establishment. I am grateful to Ms. Meni Arai at Kyoto Univ. for technical support. I am grateful to Dr. Akitsu Hotta at CiRA for technical instructions and providing basic vectors for gene-correction study. I thank Dr. Kohei Hamanaka at Yokohama City Univ. and Dr. Hiroaki Mitsuhashi at Tokai Univ. for constructive discussion. I thanks Dr.

Takashi Ikeda at CiRA and Dr. Masaki Yagi at CiRA for technical instruction. I thanks Editage (www.editage.jp) for English language editing.

Finally, I am especially grateful to my parents and family for varieties of supports and appreciate Mrs. Nao Sasaki, my wife, for her generous and unwavering support.